

AN ABSTRACT OF THE THESIS OF

Thomas Heilig for the degree of Master of Science in

Electrical and Computer Engineering presented on

June 1, 1984

Title: Design and Simulation of a Model for Lymphocyte

Flow Through Single Lymphnodes

Abstract approved: _____

Redacted for privacy

~~_____~~
R. R. Mohler U U ✓

A compartmental model of lymphocyte circulation through a lymphnode is derived and simulated. The purpose of the model is to analyze experimental data and in turn design experimental plans from the analysis in order to obtain sufficient data for the organ-distributed immune response. The model will be used to predict and analyze lymphocyte migration kinetics within a lymphnode as well as the output of lymphocytes from a node into efferent lymph. The importance of such a model is discussed in Chapter I together with a review of past models in theoretical immunology. Chapter II summarizes the immunological theory the model is based upon. A summary of the theory of compartmental analysis is given in Chapter III. A compartmental representation based on

physiological theory is derived. The mathematical model based on compartmentation and lymphocyte kinetics is derived in Chapter IV. The constants for the model are evaluated for the rat. A computer simulation of the model is performed and discussed in Chapter V. Results of the simulation are compared to literature data and predictions for lymphocyte kinetics in compartments of a lymphnode are presented. Further experiments are necessary to verify the model. A proposal for an experimental design is presented together with a predictive analysis of simulation results for the proposed experiment. It is concluded that integrated research consisting of experimentation, mathematical analysis, model development and computer simulation eventually may lead to a better understanding of the immune process and its role in disease control.

DESIGN AND SIMULATION OF A MODEL
FOR LYMPHOCYTE FLOW THROUGH SINGLE LYMPHNODES

by

Thomas Heilig

A THESIS

submitted to

OREGON STATE UNIVERSITY

in partial fulfillment of
the requirements for the
degree of

Master of Science

Completed June 1, 1984

Commencement June 1985

APPROVED:

Redacted for privacy

Professor of Electrical and Computer Engineering
in charge of major

Redacted for privacy

Head of Electrical and Computer Engineering Department

Redacted for privacy

Dean of Graduate School

Date thesis is presented June 1, 1984

Typed by researcher for Thomas Heilig

TABLE OF CONTENTS

I. INTRODUCTION	1
Previous Work	3
II. IMMUNOLOGICAL THEORY	5
Architecture of Lymphnodes	5
Lymphnode Compartments	9
Lymphocyte Population	12
T Cell Circulation	12
B Cell Circulation	13
Entrance from Lymph	14
Antigenic Stimulation	16
III. COMPARTMENTAL SYSTEM	17
Theory of Compartmentation	17
Derivation of Lymphnode Compartments	21
IV. MATHEMATICAL MODEL	30
Purpose of the Model	30
Modeling of Lymphocyte Drift	33
Modeling of Lymphnode Regions	42
Restriction to Smaller Model	53
Parameter Evaluation	55
V. SIMULATION	66
Computer Program	66
Parameter Adjustment	68
Simulation Results	71
VI. CONCLUSION	90
BIBLIOGRAPHY	94

LIST OF FIGURES

Figure	Page
1. Structure of the lymphatic system	6
2. Distribution of lymphnodes in the body	7
3. Structure of a lymphnode	8
4. Pathways of lymphocytes through a lymphnode	27
5. The recirculating pool of lymphocytes	31
6. Diffusion model for lymphocyte migration	39
7. Time-delay model for lymphocyte migration	41
8. Model for high endothelial walls	43
9. Model for superficial sinuses	44
10. Model for sinus walls	45
11. Diffusion model for interfollicular interstitium	47
12. Time-delay model for interfollicular interstitium	48
13. Diffusion model for paracortical nodules	49
14. Time-delay model for paracortical nodules	50
15. Diffusion model for follicular nodes	51
16. Time-delay model for follicular nodes	52
17. Model for medullary sinuses	53
18. Complete model for lymphocyte migration from blood to lymph across a lymphnode	62
19. Comparison of literature data and simulation results	69
20a. Simulation results I for laboratory experiment	72

20b.	Simulation results II for laboratory experiment	73
21a.	Simulation results I for step-input	76
21b.	Simulation results II for step-input	77
22a.	Simulation results I for input set to 0 at 120 minutes	79
22b.	Simulation results II for input set to 0 at 120 minutes	80
23a.	Simulation results I for bolus input	81
23b.	Simulation results II for bolus input	82
24a.	Simulation results I for exponential input	84
24b.	Simulation results II for exponential input	85
25a.	Simulation results I for linear decreasing input with constant limit value	86
25b.	Simulation results II for linear decreasing input with constant limit value	87

LIST OF TABLES

Table		Page
1.	List of Variables	64
2.	List of Constants	65
3.	Parameter values	89

Design and Simulation of a Model for Lymphocyte Flow Through Single Lymphnodes

I. INTRODUCTION

Computer modeling and simulation has evolved in parallel with the development of modern high speed computers and it has become a powerful tool with almost unlimited potential.

Systems theory was originally developed by engineers and mathematicians as a tool in the analysis of engineering problems. Applied to the wide field of immunology it proved to be a very useful method to reduce the complex concepts of the immune process to its essential mechanisms and thereby provide a better understanding of the entire system.

Cooperation between experiment and systems analysis will result in a deeper understanding of the principles of the immune process. Modeling and identification theory are tools to analyze experimental results and thereby provide a more precise knowledge as well as a quantitative description of a given system. New hypotheses can be established and tested in a model and experiments can be designed in a more focussed manner to test a predicted behavior.

The purpose of this study is to develop a model for lymphocyte flow through single lymphnodes. Experimental research in this area has been rather diverse and mostly qualitative in nature. A comprehensive study of the underlying mechanisms will be useful in directing further experimentation to areas where more data is needed.

Compartmental analysis was chosen for this study as the most useful concept for the analysis of tracer experiments.

A lymphnode can be physically divided into several regions with respect to their content of recirculating lymphocytes. These regions can be designated as compartments for further analysis.

Compartmental analysis is a powerful method in a pathway study because of its flexibility and its closeness to actual physical processes. It can be easily adapted to a wide range of applications.

Finally, model building should not be regarded as an endpoint in itself, but rather as a useful tool for testing and judging the viability of theoretical concepts.

PREVIOUS WORK

System analysis in immunology has found increasing interest in the last two decades. The first step was marked in 1966 by Hege and Cole [28] with a preliminary analysis and a first model for circulating antibodies. Jilek and Sterzl [33,34] followed with a Poisson stochastic model in 1971, describing development of the antibody-producing cell.

Bell [3,4,5] derived more advanced models based on antigen-antibody binding and the clonal selection theory by Burnet [9]. Bruni et.al. [7,8] extended this concept by deriving a distributed dynamical model of the immune response which includes a theoretical examination of the system structure.

Compartmentation and T-B cell interaction was studied by Mohler and his co-workers [44,45,46,47,48]. They also introduced the concept of bilinear systems in immunology.

Hammond [33] based his compartmental analysis of the spleen on a very comprehensive laboratory-study by Ford et. al. [19] and he introduced marginal zones, red and white pulp zones as compartments. He used an analog computer for his simulation and his approach is probably the closest work to the study presented here.

A non-linear model of the humoral immune response with a discrete time-lag was introduced by Dibrov et. al. in 1976 [14].

Extensive overviews of the state of the art in theoretical immunology are given by Marchuk [41] and Mohler [49].

Compartmental system analysis is widely used in pharmacokinetics and this was also the field where the first major application of compartmental analysis was introduced by Teorell [61] in 1937. The term 'compartment' however was not introduced until 1948 (by Sheppard [55]).

II. IMMUNOLOGICAL THEORY

ARCHITECTURE OF LYMPHNODES

Lymphnodes are the only lymphoid organs placed in the course of lymphatic vessels. While tonsils, spleen and thymus have only efferent lymphatics, lymphnodes have both afferent and efferent lymph vessels [63]. Lymphnodes are the entrance-port for lymphocytes crossing from blood to lymph. Very few lymphocytes are found in the afferent lymph before it has passed through lymphnodes.

The structure of the lymphatic system is shown in Figure 1. The arrows indicate pathways of lymphocyte migration. Lymphocytes are circulated throughout the body with the bloodstream. Lymphatic vessels collect cells which left the blood in the tissues. Consequently these cells are passed by lymph through a chain of lymphnodes before returning to the blood in the thoracic duct. Lymphocytes also find their way into lymph by entering lymphnodes directly.

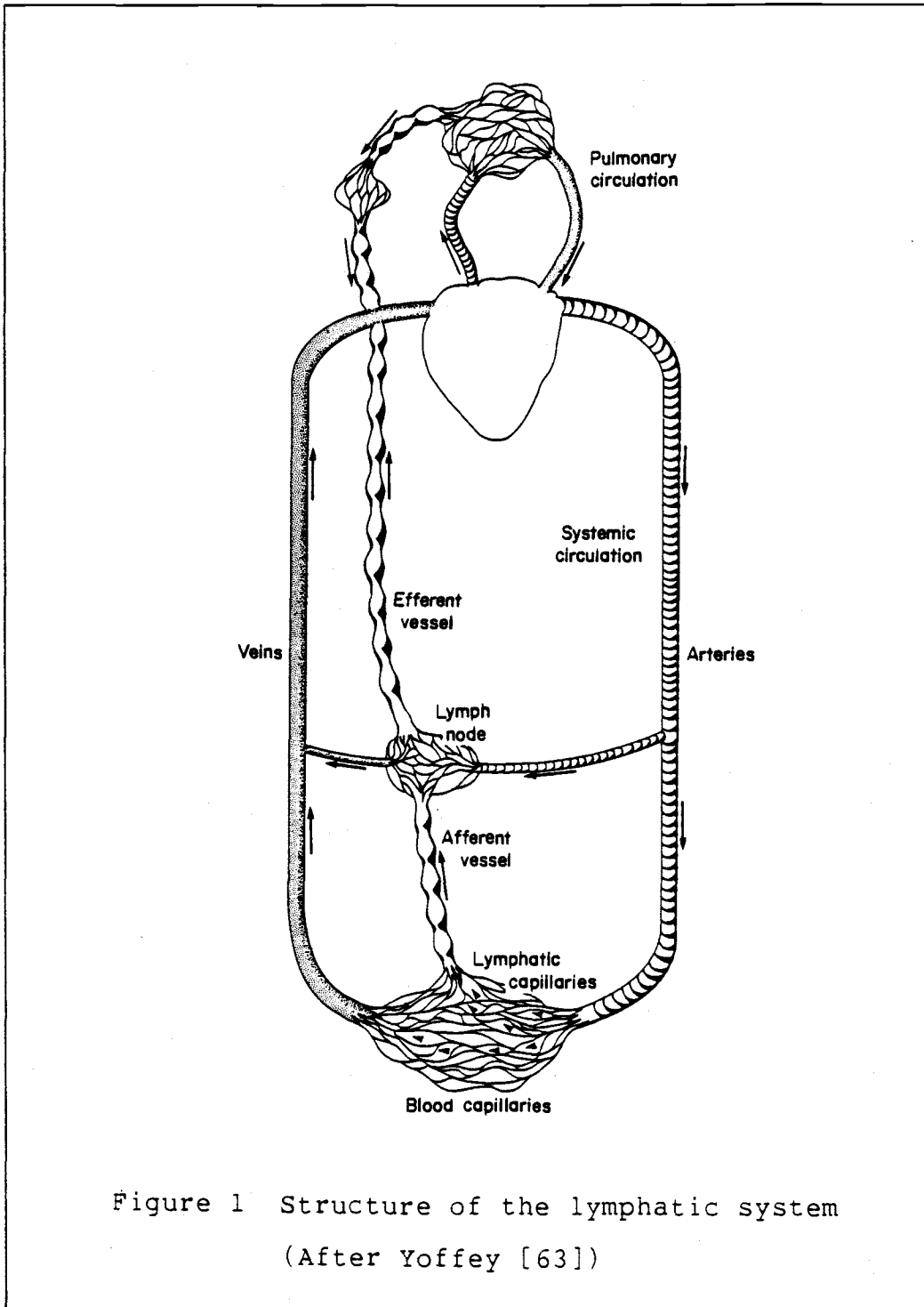


Figure 1 Structure of the lymphatic system
(After Yoffey [63])

A large number of lymphnodes are distributed all through the body as illustrated in Figure 2.

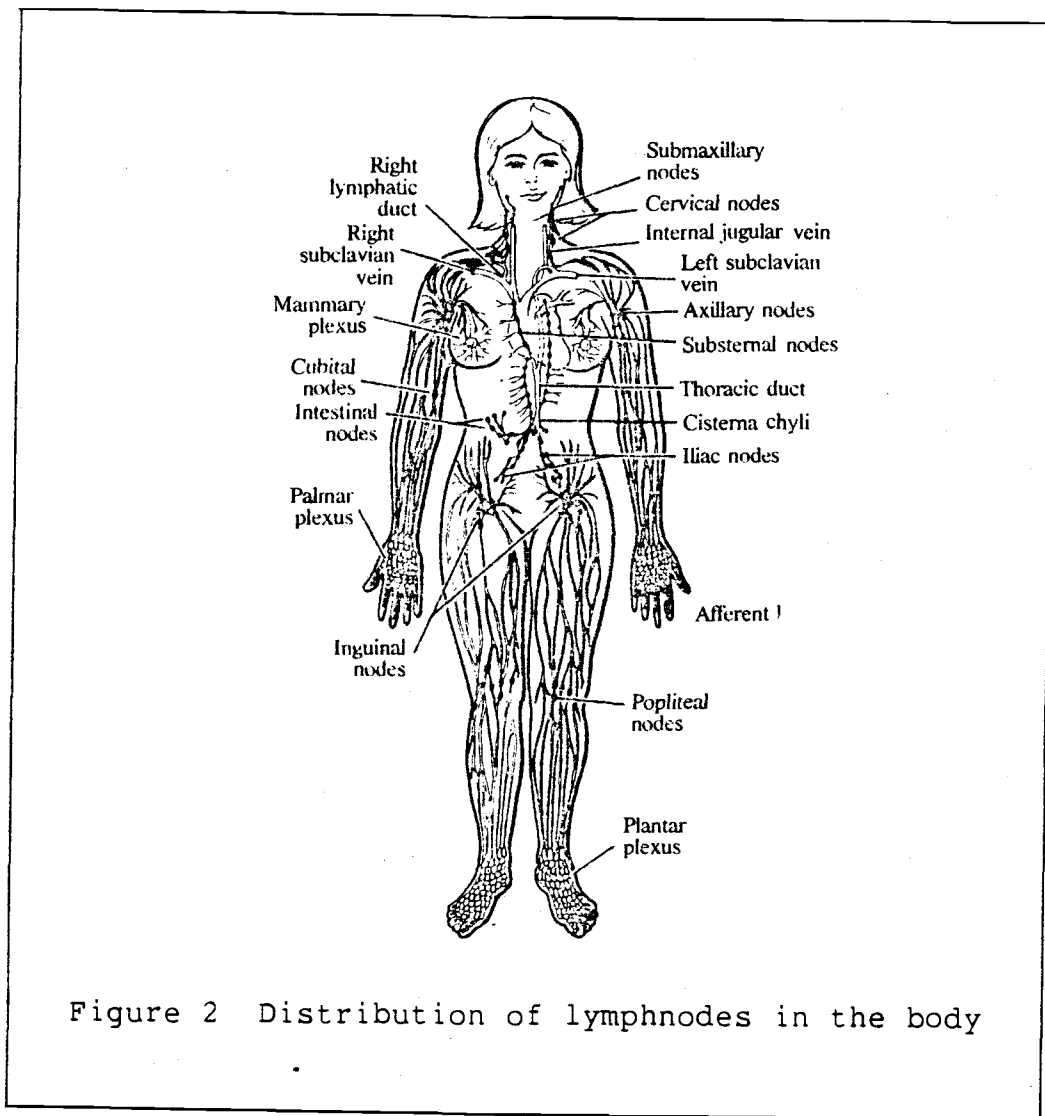
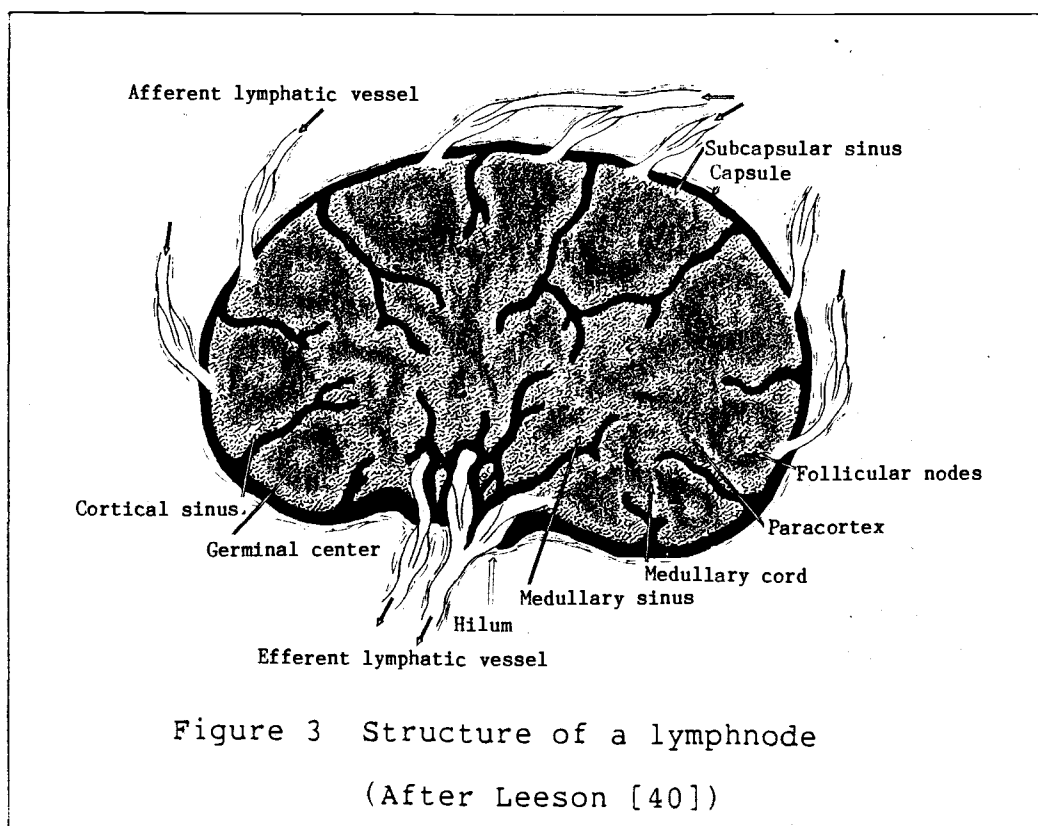


Figure 2 Distribution of lymphnodes in the body

Frequently they are found in chains or groups. A single node is an oval or bean-shaped body from 1 to 25 mm in diameter. A diagram illustrating the structure of a lymph node is given in Figure 3. The outside is covered by the capsule, continuous connective tissue that extends

with a number of trabeculae into the inside of the organ. The inside consists of two major regions, the outer cortex and the inner medulla. The cortex is characterized by the presence of lymph nodules, while the medulla consists of lymphoid tissue arranged in irregular cords.



Lymphatic vessels enter the node at multiple points on the convex side of the capsule. After piercing through the capsule, these vessels open into a system of lymph sinuses, a large network of thin channels through which the lymph percolates to finally reach the efferent lymphatic vessels, situated at the hilum of the node.

Blood vessels enter and leave the node through the hilum. After entering a node, arteries branch into the medulla and continue into the cortex to supply cortical nodules. Capillaries in medulla and cortex collect blood for postcapillary venules (PCV). PCV that are lined by a thick, continuous endothelium are called high endothelial venules (HEV). Lymphocytes enter a node from blood by penetrating high endothelial walls (HEW) of PCV [54]. Postcapillary venules then open into veins, leaving the node again through the hilum.

LYMPHNODE COMPARTMENTS

Lymphocyte traffic through the different regions of lymphnodes has been examined in many experiments, but still little is known about the effects responsible for the observed migration patterns. A systematic pathway study might lead to a better understanding of these effects. A precise function should be assigned to each tissue compartment in order to determine

- i. the site of B and T cell interaction,
- ii. the site of antigen localization,
- iii. the site at which macrophages appear,
- iv. the presence of macrophages.

The lymphnode is conventionally divided into superficial cortex, deep cortex and medulla. These regions however merge gradually into each other and are

not divided by clear borders. This makes them inappropriate candidates for compartments of a pathway study.

Fossum [20] suggests to divide the node into sinuses, interstitium and germinal centers. In contrast to cortex and medulla these compartments are clearly separated by continuous borders.

Sinuses can be subdivided into superficial and deeply situated parts. Superficial sinuses include the sinuses of the superficial cortex and the subcapsula. They are lined by a high endothelium which is continuous except for cells penetrating the walls. Only a low population of lymphocytes is found in superficial sinuses, while there are quite a few macrophages present [13]. Lymphocytes enter the node from lymph by crossing the walls of superficial sinuses. Deeply situated sinuses are lined by a flat endothelium, no complete basement membrane exists. All cells are found in the lumen, not in contact with the walls, which shows that there is no exchange of cells between lymph and lymphnode in this region. Medullary sinuses finally are the site of re-entry of lymphocytes into the lymphatic stream. The sinus network recombines to efferent lymphatics.

The interstitium can be subdivided into follicles, paracortical nodules, interfollicular interstitium and

medullary interstitium. These subregions are defined by a different composition of cells. The primary follicles are areas where B-cells locate in the lymphnode. They contain only few non-lymphoid cells, some fibroblast/reticulum cells and almost no macrophages or interdigitating cells. Paracortical nodules are single large areas ranging deep into the superficial cortex. The border to medulla or follicular interstitium is not clearly defined. T-cells concentrate here and cells migrating into the lymphnode penetrate the high endothelium in the vicinity of these nodules. The interfollicular interstitium is the region where cells from blood or lymph first enter the lymphnode via penetrating the walls of HEV. Both T-cells and B-cells are present, though B-cells migrate to primary follicles and lymphocyte corona in the superficial cortex, while T-cells either remain here or migrate to paracortical nodules. The medullary interstitium surrounds medullary sinuses. Medullary cords are included in this area.

Germinal centers are areas sharply demarcated from the surrounding corona. The cell population contains medium-sized and large lymphocytes, cells in mitosis and tangible body macrophages. Almost no recirculating lymphocytes are found here. Germinal centers will therefore be of minor importance for this study.

Lymphocyte Population

The existence of two major classes of lymphocytes being functionally and developmentally distinct has been established. Both cell types are derived from bone marrow, but T cells, in contrast to B cells, are processed by the thymus before they enter the recirculating pool [27,28,32]. The different populations show selective migration within the circulatory pool [35,60]. Different surface properties are assumed to be responsible for this phenomena.

T and B cells enter the lymphnode both the same way, by crossing the walls of HEV [54]. After entering the node, T cells either remain in the paracortex surrounding the HEV or move to paracortical nodules nearby [17,26,53]. B cells migrate to primary follicles and to the lymphocyte corona in the superficial cortex [52].

T Cell Circulation

Most of the experiments with lymphocytes have been done with T cells, because they are easily radioactively labelled. T cells have been found to cross HEV in an average time of about 6-10 minutes. They remain in the paracortical area for several hours. After crossing HEV they appear first in the interfollicular interstitium of the paracortex. It takes approximately two hours before

the first cells have entered paracortical nodules.

From the paracortical area T-cells move on to medullary sinuses. Nothing is known about the path they take. After entering the medullary sinuses, they are washed out by the efferent lymph. The average transit time for T cells from blood to lymph is given to be approximately 12 hours [58]. About 90% of the T cells in a resting node are found in the paracortical area, around 1-1.5% associated with HEV and some 6-7% in medullary sinuses. Superficial sinuses of a peripheral node contain approximately 1% of the total lymphocyte population in the node [57].

B CELL CIRCULATION

A comprehensive study by Nieuwenhuis and Ford [52] on B cell circulation through lymphnodes of a rat showed the following results: Radioactively labelled B cells were injected into the blood of a recipient and their appearance in different parts of the lymphnode was observed at several time intervals.

At 15 min after injection, labelled cells were found in the walls and immediately around HEV. At 1 hr after injection, some had crossed the walls and were scattered throughout the paracortex, without showing any tendency to localize in the superficial cortex. At 3 hrs, most

cells still were found in the paracortex, though they started showing some tendency moving towards the base of primary follicles. Primary follicles are the homing region of B cells in a lymphnode. At 6 hrs after injection, most labelled cells had already reached the base of primary follicles, a few were found in the lower part of the lymphocyte corona. At 18 hrs after injection, the labelled cells were evenly distributed around the lymphocyte corona and in primary follicles of the superficial cortex, only very few were found inside a germinal center. This pattern persisted up to the end of the test period at 48 hrs. Non-stimulated B-cells remain in the B-region of the lymphnode for many hours before they return to the medulla and are washed out by efferent lymph. B cells take approximately 2-3 times as long as do T cells to migrate from blood to lymph through a lymphnode.

Even though this is probably the most detailed and comprehensive study on B-cell circulation through lymphnodes so far, it is mostly qualitative and reveals little quantitative data.

ENTRANCE FROM LYMPH

The migration of lymphocytes from lymph into lymphnodes has received less attention than the entrance from blood, but some important features of this

alternative path have been explored in recent years.

Afferent lymph first enters a lymphnode in the superficial sinuses below the capsula. From here lymphocytes can take two different routes. They either enter the node by penetrating the endothelium of the sinuses or they remain within the lumen, pass on to deep sinuses and consequently leave the node via medullary sinuses without having entered [20,39]. The relative proportions of lymphocytes entering a lymphnode from blood or from lymph depends on the location of the lymphnode within the lymphatic chain [18]. In peripheral lymphnodes the percentage of lymphocytes entering the node from lymph is less than 10%, while 90% arrive from the blood [31].

The proportions in central nodes are very different and a recent study postulates that the number of lymphocytes entering the node from the blood may be regulated by the number of lymphocytes in the afferent lymph [61]. The possibility of lymphocytes entering the blood directly from lymph through lymphnodes ('direct entry') was reported for some species. However, more recent experiments concluded that this pathway does not exist [1,63].

ANTIGENIC STIMULATION

After antigenic stimulation by a thymus-dependent antigen, plasmablasts (activated B cells) appear at the border between deep and superficial cortex, diverted from their course toward the lymphocyte corona. They appear to migrate along the outer edge of the paracortex towards the medulla, where they remain in medullary cords as plasma cells or leave the node via efferent lymph [20].

Activated T lymphocytes are immobilized in the paracortex for several days. Since B and T cells both enter the node in the paracortex, this is most probably the site of T-B interaction in an immune response [13].

Among the first observed effects of a stimulation with different antigens are the decrease in the output of both B and T lymphocytes via the efferent lymph and the increase of lymphocytes around postcapillary venules, probably reflecting a greater uptake of lymphocytes by the node . This effect is known as the 'shutdown' of lymphnodes during the first stages of an immune response [41]. The level of lymphocytes around HEV remains above normal for about a week after stimulation [23].

III. COMPARTMENTAL SYSTEM

THEORY OF COMPARTMENTATION

Jacquez [36] defines a compartmental system as " a system which is made up of a finite number of macroscopic subsystems, called compartments or pools, each of which is homogeneous and well mixed, and the compartments interact by exchanging material". A compartment is defined by Brown [7] as " a vessel which contains a single form of matter (or energy), and to which the law of conservation of matter (or energy) applies".

One of the most useful applications of compartmental analysis lies in the examination of tracer experiments. "The tracer method is a technique for observing a population of specific things such as molecules, living creatures, or other entities by a process of labeling" is the definition given by Sheppard [57].

Quite often it is impossible to measure quantities and their dynamic behavior in a system directly. By introducing a small amount of labeled material into the system and following its dynamic distribution however it is sometimes possible to get a quite accurate description of the actual behavior of a system. The standard procedure is to inject labeled material into one compartment. At different time intervals, samples from

this and other presumed compartments are obtained and analyzed.

A number of conditions must be satisfied to assure viability of the tracer method

- i. The system must be in steady state
- ii. There is complete mixing of labeled and unlabeled material in each compartment and the mixing occurs rapidly with respect to the transfer rates between compartments.
- iii. The amount of labeled material injected into a compartment is small compared to the total amount of examined substance in this compartment; that is, it is in fact a 'tracer' amount.
- iv. The labeling does not in any way affect the migration properties of the examined substance.
- v. To further simplify the analysis, we assume the system to be conservative, which means we assume that no cells of our observed pool die or are newly born. This assumption can be justified since we are dealing only with recirculating lymphocytes which are known to be longlived. Also included in this assumption is that we will not consider any loss of labeled material by radioactive decay

within the observed timespan.

From these principles the theory of compartmental analysis of tracer systems can be developed. An extensive derivation is given in references [36,56]. Only a short summary of the results will be given here.

Consider a compartmental system obeying the basic mass conservation law, which states that the change of mass in any given region is equal to the sum of all influxes minus the sum of all outfluxes.

$$\frac{dS_i}{dt} = \sum_{\substack{j=1 \\ j \neq i}}^n F_{ji} - \sum_{\substack{k=1 \\ k \neq i}}^n F_{ik} + F_{oi} - F_{io}, \quad (1)$$

where S_i is the amount of substance S in compartment i , F_{ij} is the mass flow of this substance per unit time from compartment i into compartment j ; F_{i0} consequently denotes the flow from compartment i to the environment while F_{oi} stands for flow from the outside world into the i th compartment.

We consider the total amount of S as constant, or in other words, no new material is produced nor is any destroyed. Assume that at time $t=0$ we inject some tracer amount of labeled material into one or more compartments of this system. The total activity in the i th

compartment will be denoted by R_i . The labeled fraction R_i/S_i will be the specific activity A_i .

If conditions ii-v as given above apply, i.e. the tracer is uniformly distributed throughout substance S, migration properties are not affected by the labeling, and both death and birth rate are zero, the kinetic behavior of the tracer system can be described by the general equation

$$\frac{dR_i}{dt} = \sum_{\substack{j=1 \\ j \neq i}}^n F_{ji} \cdot A_j - \sum_{\substack{k=1 \\ k \neq i}}^n F_{ik} \cdot A_i + F_{O_i} \cdot A_O - F_{iO} \cdot A_i. \quad (2)$$

From equation (1) and (2) we can derive the equation for tracer specific activities, making use of the relation $R_i = S_i \cdot A_i$.

$$\frac{dA_i}{dt} = \sum_{\substack{j=1 \\ j \neq i}}^n (F_{ji}/S_i) \cdot (A_j - A_i) + (F_{O_i}/S_i) \cdot (A_O - A_i).$$

The significance of this result is that the obtained system is linear in specific activity. If we assume further that the system is in steady state, which means $dS_i/dt = 0$ and the flow rates F_{ij} are constant for all i, j , we obtain for the specific activity

$$\frac{dA_i}{dt} = (1/S_i) \cdot \left\{ \sum_{\substack{j=1 \\ j \neq i}}^n F_{ji} \cdot A_j - \sum_{\substack{k=1 \\ k \neq i}}^n F_{ik} \cdot A_i + F_{oi} \cdot A_o - F_{io} \cdot A_i \right\}.$$

The rates of exchange in this system are now constant and can be derived from the often measurable steady state distribution of the tracer. The importance of this result can hardly be overestimated since it forms the basis for many applications of the tracer method.

DERIVATION OF LYMPHNODE COMPARTMENTS

Another reason for choosing a compartmental approach is its flexibility. The node can be divided into several physical compartments with respect to their lymphocyte population. In a next step, these compartments will be further divided into subcompartments to model the specific behavior of each region. This approach has the advantage that the subcompartmentation can be easily changed in the progress of model-development. Several possibilities to mimic the kinetic character of each area can be tested without changing the overall composition of the model. While the macro-compartments correspond to physical locations in the node, the subcompartments are nothing more than mathematical images of certain physiological effects and have nothing to do with any physical locations within the large compartment.

As was described previously, lymphocytes leave the blood in postcapillary venules of a node. They enter the high endothelium of PCV and migrate through intercellular spaces towards the paracortex.

In this model, we consider the blood in PCV as part of the environment, not as part of the lymphnode itself. The concentration of lymphocytes in the blood is dependent on many other organs. Since this study is dealing only with lymphnodes, we are looking at an open system. Lymphocytes enter the node from blood and from afferent lymph and leave again with efferent lymph. Lymphocyte concentration in blood and lymph therefore has to be given as an input to the system. Blood will be considered as a steady and continuous supply of lymphocytes, and uptake by the node does not change the local concentration of lymphocytes in PCV.

The High Endothelial Walls of PCV will therefore be taken as the first compartment of the lymphnode, they are the port for lymphocytes entering the node from blood. After crossing HEW, lymphocytes appear in the interfollicular interstitium of the paracortex. Here they are joined by cells having entered the node by a different way.

Lymphocytes also can enter a node from lymph. Though only a small portion of the total lymphocyte

population in a node come from lymph, this pathway has been well established [11,20]. Afferent lymph enters the node through the capsula and drains into subcapsular sinuses. Some of these sinuses, usually near the paracortical area, are lined by a high endothelium, which lymphocytes are able to penetrate. After crossing sinus-walls, lymphocytes appear in the interfollicular interstitium, where they join the cells having entered from blood.

The interfollicular interstitium in the paracortex is therefore a compartment where two pathways join (from lymph and from blood) and where two other streams diverge (B cells and T cells migrate from here to different areas). B and T cells have been migrating together up to this point in the node, but here a division occurs. B cells migrate towards primary follicles of the outer cortex, while T cells remain in paracortical nodes of the paracortex. Not much is known about the forces responsible for this division. While it seems to be well established that certain surface receptors that are present on both B and T cells are responsible for their migration across HEV [30,60], several possibilities are considered to be effective for their selective migration into different areas in the node.

Weissman et.al. [62] speculate about the following

possibilities: There might exist microscopic pathways within lymphoid tissue for the two different cell types. Each cell type would recognize its own pathway and follow it to the respective homing areas. No such structure has been found so far. Another reason for the selective migration of T and B cells could be different kinds of chemotaxis for each subpopulation. Distinct chemotactic substances could be produced locally and attract only the appropriate cell type.

A third hypothesis is the existence of distinct microenvironmental properties for follicles and paracortical nodes. T cells might find their migratory capacity greatly diminished after having entered a paracortical node, while B cells would continue to move until getting stuck in primary follicles. Finally there is the possibility of a cell type attracting only companions of the same type. A B cell having more or less randomly entered a follicle would then in turn attract other B cells. All these are presently nothing more than speculations, but they illustrate the wide range of possibilities and also the almost complete ignorance in this particular field.

A majority of T cells remain immobilized in paracortical nodules for several hours. Thereafter they reappear again in the medullary sinuses from where they

are washed out with the efferent lymph. The path they take from paracortex to medullary sinuses is not known [62]. A similar characteristic applies for B cells in their respective area of the node. They remain immobilized in primary follicles for an even longer time than T cells. Again on paths that are not known they eventually return to medullary sinuses to recombine with T cells and subsequently be flushed out by efferent lymph.

A complete diagram of lymphocyte pathways through a lymphnode is given in Figure 4. The lymphnode has been divided into several regions each of which has a specific task with respect to lymphocyte migration. A summary of these regions and their particular tasks is given below.

Superficial sinuses - site of entrance of cells from lymph. Division into two streams, one entering the node, a second one remaining in lymph.

Sinus walls - the region cells have to enter and cross to migrate into the paracortex.

HEW - the region cells have to enter and cross on their way from blood into the paracortex.

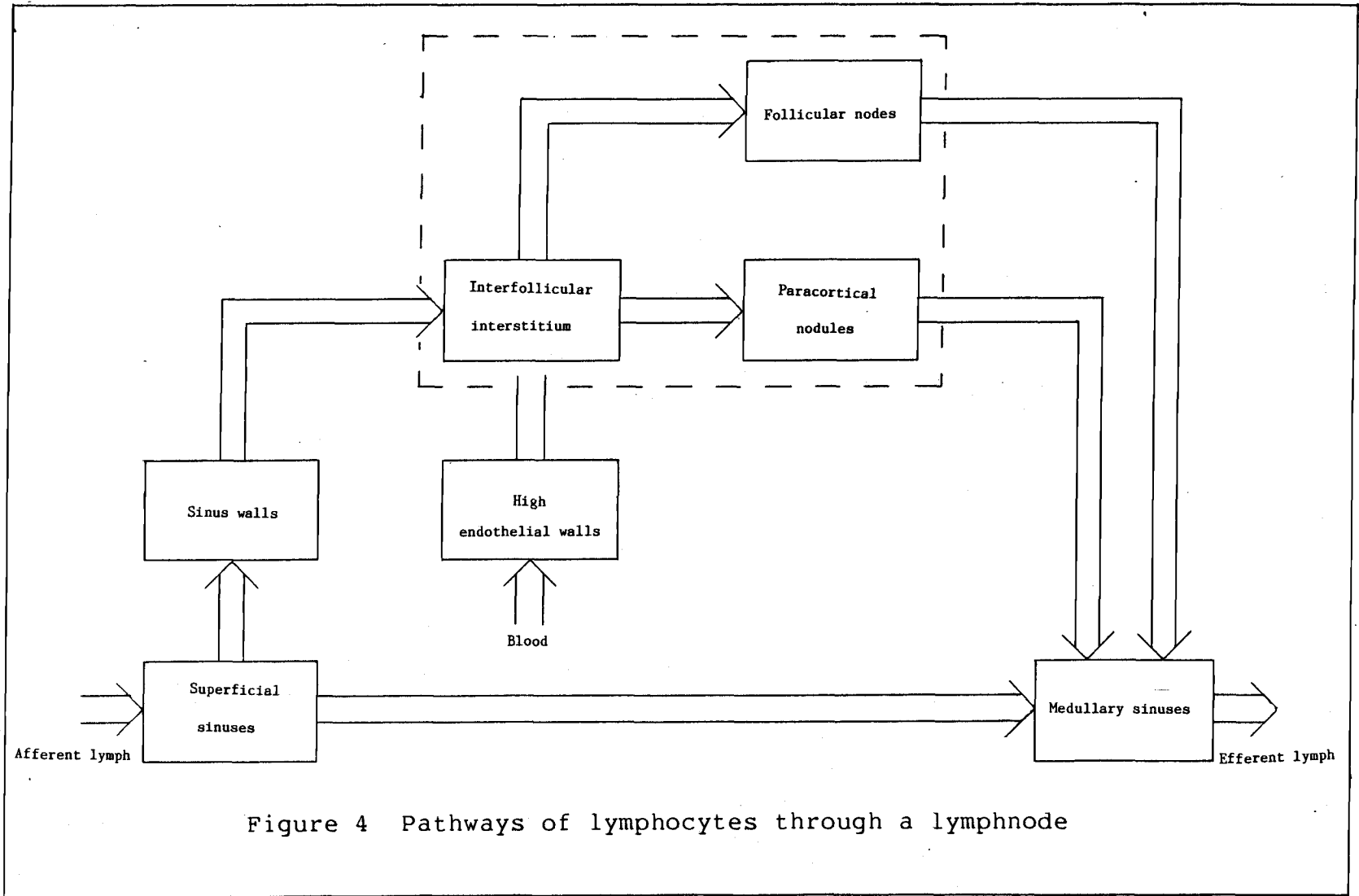
Interfollicular interstitium - the part of the paracortex where cells enter the node from the

walls of superficial sinuses and PCV. Site of T-B cell interaction in the node.

Paracortical nodules - Homing region of T cells in a node

Follicular nodes - Homing region of B cells in a node

Medullary sinuses - Site of re-entrance of lymphocytes into lymph. Exit-port for lymphocytes leaving the node.



Key to Figure 4

The following subscripts are used in Figure 4 as well as throughout this entire study

bl	blood
al	afferent lymph
el	efferent lymph
hw	high endothelial walls of PCV
ss	superficial sinuses
sw	walls of superficial sinuses
ii	interfollicular interstitium
pn	paracortical nodules
fn	follicular nodes
ms	medullary sinuses

Also used in Figure 4 are terms of the form

F_{aa-bb} flow from area aa to area bb where the

subscripts from above are used for aa

and bb

IV. MATHEMATICAL MODEL

PURPOSE OF THE MODEL

A diagram illustrating the complete recirculating pool of lymphocytes is shown in Figure 5. Lymphnodes are an important part of the system for several reasons. They contain a high concentration of recirculating lymphocytes. They are a site of T and B cell interaction during an immune response. They are also a region where antibodies are produced. For all these reasons it is important to know more about lymphocyte distribution within a lymphnode. Unfortunately lymphocyte concentrations in single regions of a node are very difficult to measure. It is possible, however, to measure the total number of lymphocytes in a node. There are also a few indications about their distribution within the node, but almost no concrete data is available. This is the point where a mathematical model can provide answers which can not be obtained experimentally.

As can be seen from Figure 5, lymphnodes are an important building block of the circulatory system.

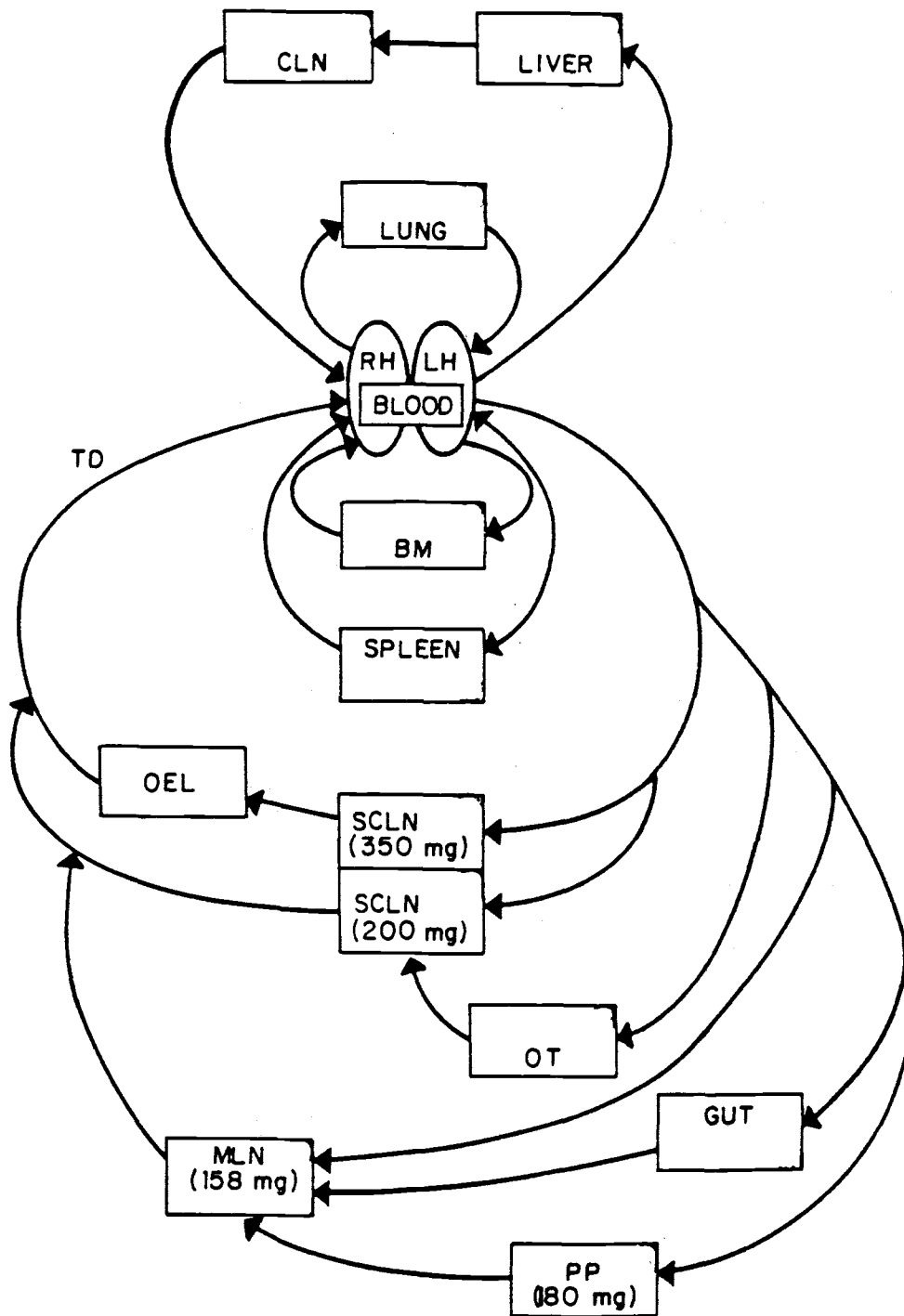


Figure 5 The recirculating pool of lymphocytes
 (After Ford, personal communication 1983)

Key to Figure 5

TD	Thoracic Duct
OEL	Other Efferent Lymphatics
SCLM	Subcutaneous Lymphnodes
CLN	Coeliac Lymphnodes
MLN	Mesenteric Lymphnodes
RH,LH	Right, Left Heart
BM	Bone Marrow
PP	Peyer's Patches
OT	Other Tissue

What this study tries to accomplish is the development of a model for lymphnodes that can be implemented in various places of the total circulatory system. It is assumed that all lymphnodes show the same characteristics with respect to lymphocyte migration.

Every lymphnode communicates with the outside world only via blood and lymph. The assumption of an 'average' lymphnode states that all lymphnodes, regardless of their position in the body, will display the same behavior for a given input function. The input function in this case is the number of lymphocytes entering the node from blood and from lymph. If used as a building block in a larger system of the complete circulatory pool the here presented model will provide lymphocyte distribution within a node as well as lymphocyte output to the larger system for any given input from the system. For the purpose of simulation of this model, the input has to be a known function, provided by either experimental data or by a larger model as mentioned above.

MODELING OF LYMPHOCYTE DRIFT

So far we have given a purely qualitative description of the examined system. In this section we will deal with the derivation of a valid set of equations to describe the kinetic behavior of each region of a node.

The first and probably most important point to mention is that the compartments that were derived in the last chapter are not compartments in a mathematical sense as they were defined on page 18. An important condition for compartmental analysis does not apply to these physical compartments: We can not assume equal distribution of lymphocytes within these regions. Even more, we can tell positively that there will be an unequal distribution of cells within certain regions.

Consider for example high endothelial walls of PCV (Figure 4). Assume that the first labelled lymphocytes have just entered this compartment. Physically this means that they started penetrating the walls of PCV. Since these walls have some thickness d and the 'speed' of lymphocytes within the wall is small, it will take a certain time for the cells to reach the other end of the wall. In other words, the concentration will be high on the inner side of the walls, but will be low on the outer side. Only if the time to cross a particular region is small compared to the total response time of the node can this effect be neglected. The solution to this problem is a subcompartmentation of a given physical region into compartments which comply with the conditions given before. These subcompartments will be constructed such that they model the kinetic behavior of a region.

The force that moves lymphocytes across HEW (and also across other areas of the node, for that matter) is not known [19,62] We could start by assuming some kind of diffusion along a pressure gradient. Blood enters a lymphnode in arterial capillaries and leaves again in venous capillaries. The blood pressure on the arterial side is higher than on the venous side and this pressure difference causes blood flow through the node. Cells and molecules are carried through the node with blood.

Complementary surface receptors are assumed to be responsible for selective adhesion of lymphocytes to the surface of a high endothelium [30]. Lymphocytes are moved through tissue by fluid flow between capillaries and by their own ameboid motion. Chemotaxical substances may cause ameboid motion by initiating action potentials in the cell membrane [26]. High endothelial cells are known to secrete a sulphated glycolipid together with glycoprotein [2] but it remains unknown if this substance has anything to do with the transport of lymphocytes across HEW.

Returning to the principle of a pressure gradient across HEW, there are at present no techniques to measure pressure inside a post capillary venule, far less on the outer side of postcapillary walls. An even bigger ignorance characterizes the state of research on

transportational forces in other areas of a lymphnode.

What we therefore need is a different approach. Rather than trying to model some unknown mechanism from physical theory we have to use the little we know about transportational effects to get a model that describes reasonably well the overall dynamics of lymphocyte flow through lymphnodes which in turn might lead to conclusions about possibly underlying mechanisms. The compartmental scheme that was adopted allows the implementation of alternative processes by simply changing the structure of subcompartments in a region.

We have to think of lymphocyte migration across any particular area of a node not as flow through one channel, but rather as flow of many cells through a labyrinth of parallel routes. It has been shown that an impulse input of a tracer into a vascular labyrinth generates an outflow that is more or less widely distributed over time. Each cell entering a region will appear at the output after some discrete time-lag T_i . Since there are many cells on many parallel pathways involved, these times T_i will be distributed in a random manner around some average transit time T . There is no hope at this time for including such detailed factors as local vascular structure in the analysis of the system.

As explained above, the effect of temporal

dispersion of individual transit times T_i around a maximum value T can be looked upon as a random process where each time value is characterized by a probability of tracer appearing at the output. This approach was taken by several workers for blood flow through a circulatory labyrinth and is well explained by Sheppard [57].

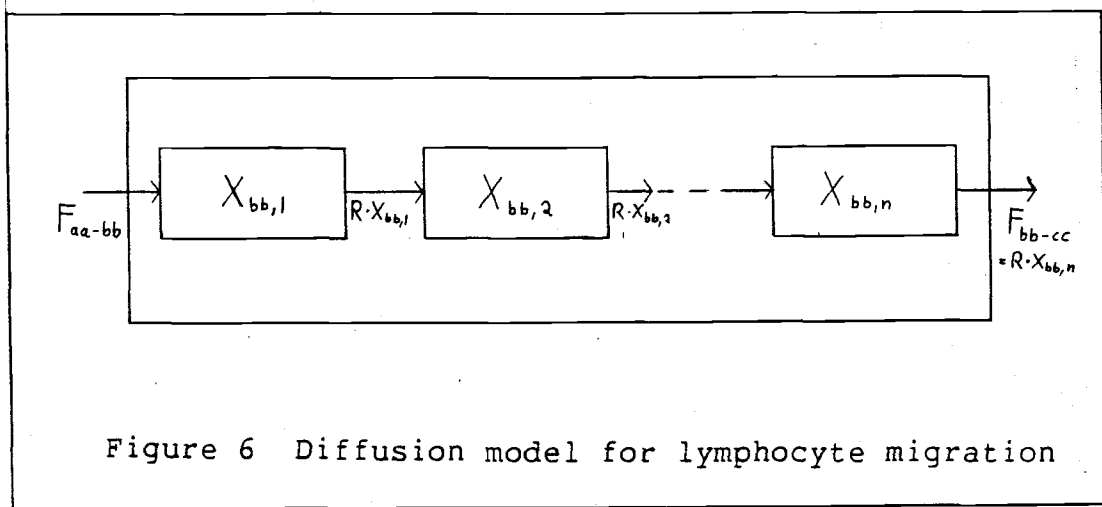
Two types of models have been considered to simulate this effect. Neither one of them has any valid physical resemblance with the actual process of multiple migrations along many parallel pathways. However, both have been shown to give a fair representation of the results of this process. So called "random walk models" consider the different stages of tracer transport through the organ as a normal distribution curve moving in horizontal direction (time) and progressively spreading out. Newman et.al. [51] are among the first to discuss a second approach that fits much better in the scheme of this study. They consider a "washout model" where label is washed through a series of well-mixed compartments. Sheppard [57] shows that the solution for a catenary series of uniformly mixed compartments of equal size has the same form as the equation for Poisson statistics.

A catenary system of compartments is conventionally used to model one-dimensional flow of a substance.

Catenary system means that compartments form a chain where input to the system can only be into the first chamber of the chain, while output is allowed only from the last compartment. Diffusion can be modeled by an infinite chain of compartments [33]. If all rate constants are equal, the process is assumed linear here. Nonlinear diffusion can be modeled by a small increase in rate constants from one compartment to the next one. Bidirectional flow processes can be superimposed by differences between forward and reverse rate constants. When the reverse rate constants become zero, the modeled process becomes equivalent to one-directional drift. This representation is mathematically equivalent to lymphocyte drift in one direction. We have stated before that lymphocyte flow in a lymphnode is one-directional; therefore this model seems appropriate. The curves that are produced by a linear catenary chain for an impulse input into the first compartment rise more or less rapidly from zero to a single broad maximum before falling far less rapidly back to zero. A fairly wide spread in curve shapes can be obtained by varying both the compartment size and the number of compartments.

Let X_{aa} denote number of cells in area aa . This state variable may be absolute number of cells or some normalized number, for example percentage of injected dose.

Suppose we want to model region bb as a linear catenary chain of compartments as described above. Input to region bb will be denoted by F_{aa-bb} , the flow from aa to bb. Output from bb will flow into region cc, as illustrated in Figure 6.



The equations for region bb are then given as

$$\frac{dX_{bb,1}}{dt} = F_{aa-bb} - R_{1,2} X_{bb,1},$$

$$\frac{dX_{bb,m}}{dt} = R_{m-1,m} X_{bb,m-1} - R_{m,m+1} X_{bb,m},$$

$$\frac{dX_{bb,n}}{dt} = R_{n-1,n} X_{bb,n-1} - R_{n,cc} X_{bb,n},$$

where

aa is the region lying before bb,

cc is the region lying after bb,

$X_{bb,m}$ is cell content of mth compartment in region bb,

$R_{m-1,m}$ is the rate constant from compartment m-1 to m,

$R_{n,cc} \cdot X_{bb,n}$ is the output from the last compartment

(compartment n) of bb to cc. It can also be

denoted as F_{bb-cc} .

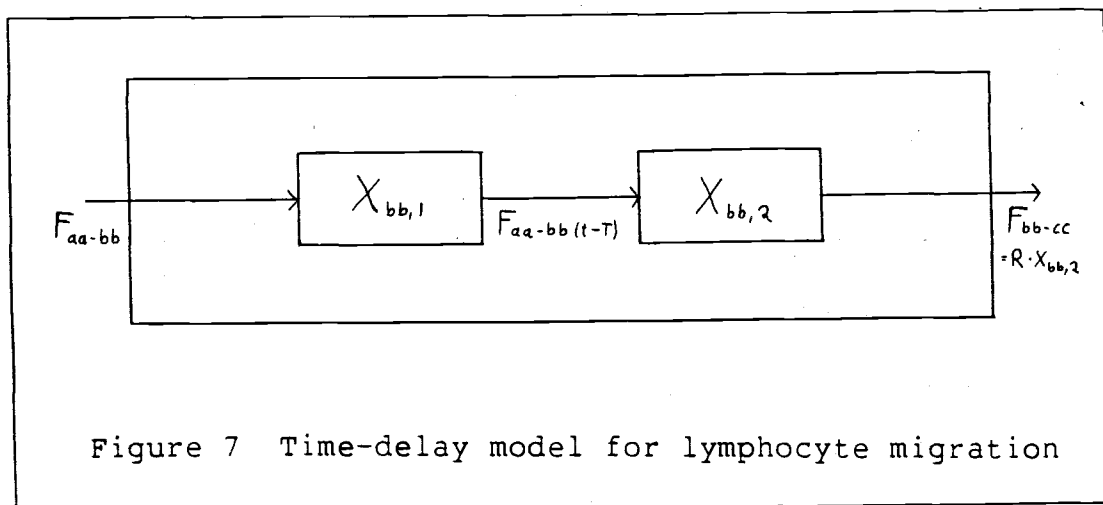
A large transit time across any given region requires a large number of compartments in the catenary chain. Under the condition that the peak in the probability distribution of transit times T_i is sharp enough, the distributed time-lag of the linear chain can be replaced by a discrete time-lag T followed by a single compartment which obeys first order kinetics and represents the spread around average transit time T . This will change the state space representation that we had before completely. The system of instantaneous differential equations where the rate of change of each variable was dependent only on its current value is replaced by delay differential equations where the previous history of a variable plays a significant role in its rate of change. Solution of a delay differential equation requires not only specification of the initial value as is the case in ordinary differential equations, but also specification of previous values over an extended time. While the initial approach of using a linear catenary chain is closer to the reality of drifting lymphocytes, the introduction of a discrete time-lag may be a reasonable approximation for regions with a long transit time. The equations for the same region bb for the representation with a discrete time-lag

can be written as

$$\frac{dX_{bb,1}}{dt} = F_{aa,bb}(t) - F_{aa,bb}(t-T),$$

$$\frac{dX_{bb,2}}{dt} = F_{aa,bb}(t-T) - R_{2,cc} \cdot X_{bb,2},$$

where T denotes a constant, finite and positive time-delay. Figure 7 shows an illustration of this concept.



Most areas with a large storage effect and consequently a long transit-time in this model will be modeled by either the model with distributed time-lag in Figure 6 or by the representation shown in Figure 7 where the distributed time-lag is lumped to a discrete transit time.

MODELING OF LYMPHNODE REGIONS

1. High Endothelial Walls

It has been well established that lymphocytes enter a node from the blood proportional to their concentration in blood (19,59) as well as proportional to the blood flow rate. Consequently we can write the flow of lymphocytes into HEW as

$$F_{bl-hw} = R_{bl-hw} \cdot Q_{bl} \cdot C_{bl},$$

where Q_{bl} is the blood flow rate (in ml/min), C_{bl} is the concentration of lymphocytes in the blood (in number of lymphocytes/ml) and R_{bl-hw} is the rate constant at which cells enter HEW from PCV, or in other words the ratio of lymphocytes entering HEW to the total number in PCV. R_{bl-hw} is a dimensionless constant.

Lymphocytes have been shown to cross HEW in an average time of 10 minutes. Compared to transit-times in the order of hours in other compartments of a node, transit time across HEW will have rather little effect on the overall kinetic behavior of the node. It seems therefore reasonable to model this region as a single compartment of first order, where the output flux is proportional to the cell content of the compartment.

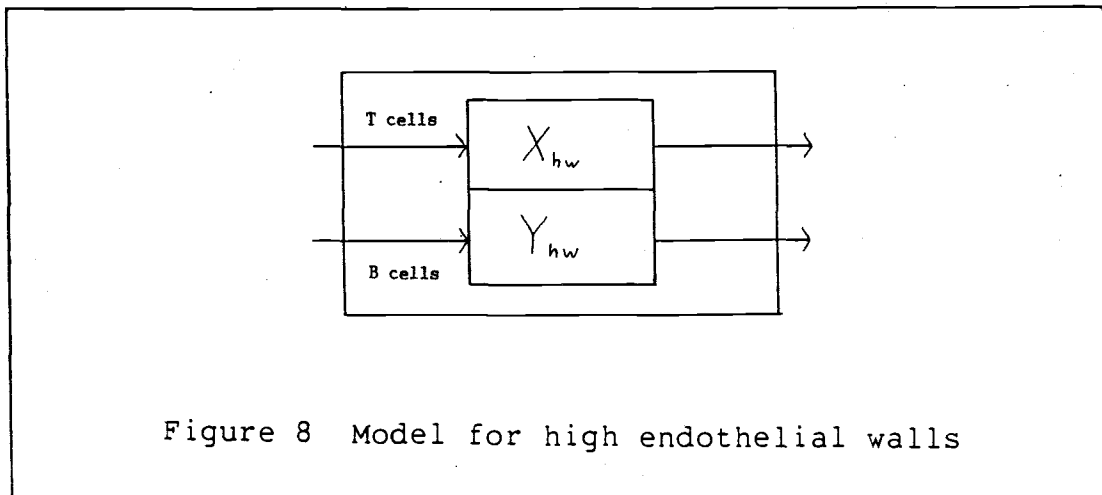
Let X_{aa} denote the amount of T cells in region aa, Y_{aa} will then be the amount of B cells in the same

region. The entire compartment will then be modeled by the following equations (see Figure 8)

$$\frac{dX_{hw}}{dt} = R_{bl-hw} \cdot Q_{bl} \cdot C_{blt} - R_{hw-ii} \cdot X_{hw},$$

$$\frac{dY_{hw}}{dt} = R_{bl-hw} \cdot Q_{bl} \cdot C_{blb} - R_{hw-ii} \cdot Y_{hw}.$$

C_{blt} denotes here the concentration of T cells in blood, respectively C_{blb} stands for B cell concentration. As mentioned before, R_{bl-hw} denotes the rate constant from blood to HEW, R_{hw-ii} is the rate constant from HEW to interfollicular interstitium.



Note that the rate constants are exactly the same, reflecting the fact that B and T cells display no difference in their transit across HEW.

2. Superficial Sinuses

Lymphocytes having entered the node with afferent lymph have to choose one out of two possible routes in

superficial sinuses. Either they remain within the sinus lumen to be carried on to medullary sinuses or they penetrate the endothelial walls of superficial sinuses and thereby enter the tissue. This is illustrated in Figure 9. The simplest approach is to look at superficial sinuses as a pool with a constant flow of lymph through it. Lymphocytes penetrating sinus walls are assumed to be proportional to the cell content of the pool. The number of lymphocytes leaving the area with lymph is of course simply their concentration in the pool multiplied by the lymph flow rate. Concentration in the pool is given by number of cells in the pool divided by the pool volume. The rate of flow of lymphocytes entering the pool will be their concentration in afferent lymph multiplied by lymph volumetric flow rate.

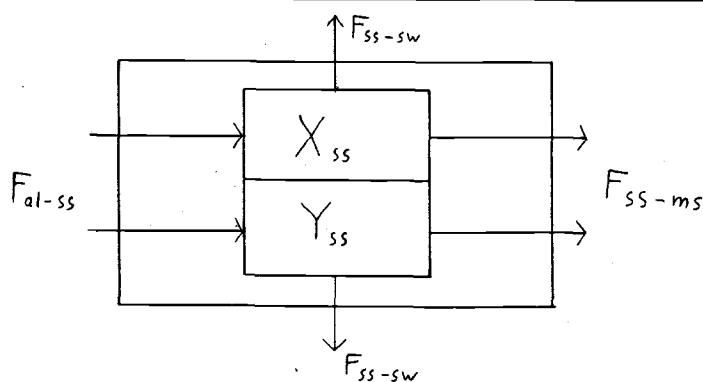


Figure 9 Model for superficial sinuses

The equation for subcapsular sinuses can now be written as

$$\frac{dX_{ss}}{dt} = Q_1 \cdot C_{alt} - R_{ss-sw} \cdot X_{ss} - (Q_1/V_{ss}) \cdot X_{ss},$$

$$\frac{dY_{ss}}{dt} = Q_1 \cdot C_{alb} - R_{ss-sw} \cdot Y_{ss} - (Q_1/V_{ss}) \cdot Y_{ss},$$

where C_{alt} and C_{alb} denote the concentrations of T and B cells in afferent lymph respectively. Q_1 is the flow rate of lymph, V_{ss} the volume of superficial sinuses and R_{ss-sw} the fractional transfer coefficient from superficial sinuses to sinus walls.

3. Sinus Walls

In the absence of any further knowledge about lymphocytes crossing high endothelial walls of sinuses, we will assume that the predominant effects are similar to those in HEW of postcapillary venules.

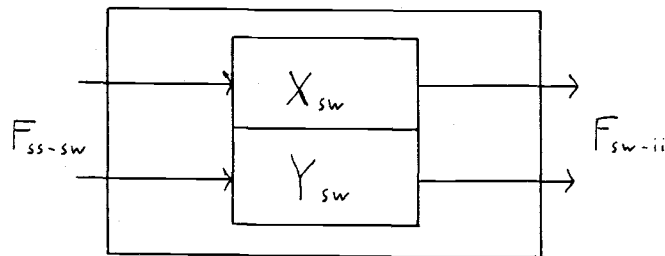


Figure 10 Model for sinus walls

We will therefore model this area like HEW, by a single compartment whose outflux obeys first order kinetics. The influx will come from superficial sinuses, as shown in Figure 10. The equations for the model are

$$\frac{dX_{sw}}{dt} = R_{ss-sw} \cdot X_{ss} - R_{sw-ii} \cdot X_{sw},$$

$$\frac{dY_{sw}}{dt} = R_{ss-sw} \cdot Y_{ss} - R_{sw-ii} \cdot Y_{sw}.$$

4. Interfollicular Interstitium

As was mentioned before, the interfollicular interstitium is the region in the paracortex of a node where entering lymphocytes from lymph and from blood come together. It is also the region where B and T cells start taking different routes through the node. Nothing at all is known about effects like pressure gradients inside this region, which is not very surprising since the region is not even well defined. Lymphocytes migrate due to some unknown mechanism through the area towards their respective homing region. But in contrast to HEW the time delay in this region is of considerable size with respect to the overall kinetics of the node. Therefore we will use one of the alternative configurations presented in the previous section. Figure 11 illustrates the 'distributed' time-lag approach.

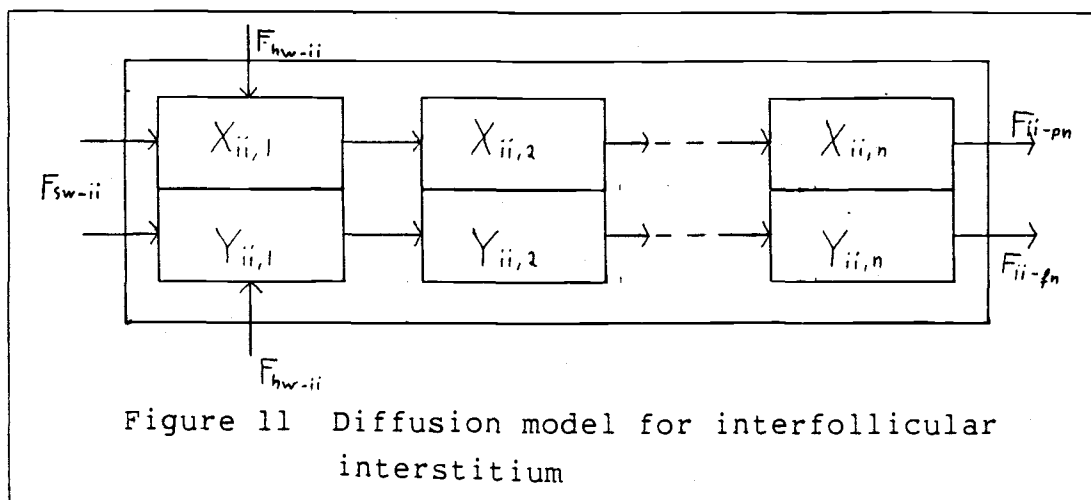


Figure 11 Diffusion model for interfollicular interstitium

The equations for this case are

$$\frac{dX_{ii,1}}{dt} = R_{hw-ii} \cdot X_{hw} + R_{sw-ii} \cdot X_{sw} - R_{ii} \cdot X_{ii,1},$$

$$\frac{dX_{ii,m}}{dt} = R_{ii} \cdot X_{ii,m-1} - R_{ii} \cdot X_{ii,m},$$

$$\frac{dX_{ii,n}}{dt} = R_{ii} \cdot X_{ii,n-1} - R_{ii-pn} \cdot X_{ii,n},$$

$$\frac{dY_{ii,1}}{dt} = R_{hw-ii} \cdot Y_{hw} + R_{sw-ii} \cdot Y_{sw} - R_{ii} \cdot Y_{ii,1},$$

$$\frac{dY_{ii,m}}{dt} = R_{ii} \cdot Y_{ii,m-1} - R_{ii} \cdot Y_{ii,m},$$

$$\frac{dY_{ii,n}}{dt} = R_{ii} \cdot Y_{ii,n-1} - R_{ii-fn} \cdot Y_{ii,n}.$$

The approach with a discrete time-lag is shown in Figure

12. The equations are

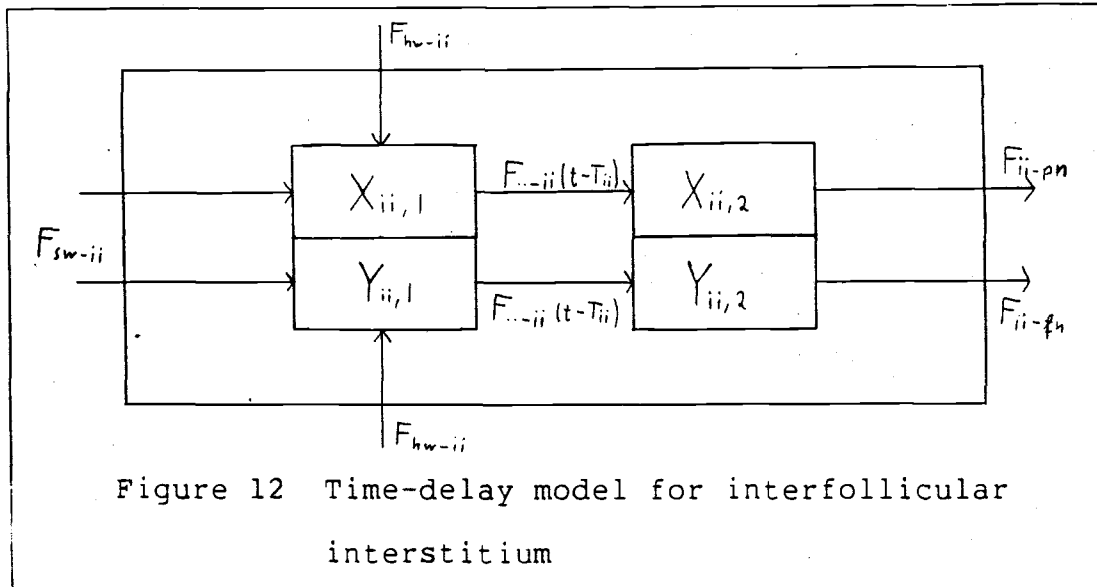
$$\begin{aligned} \frac{dX_{ii,1}}{dt} = & R_{hw-ii} \cdot [X_{hw}(t) - X_{hw}(t-T_{ii})] \\ & + R_{sw-ii} \cdot [X_{sw}(t) - X_{sw}(t-T_{ii})], \end{aligned}$$

$$\begin{aligned} \frac{dX_{ii,2}}{dt} = & R_{hw-ii} \cdot X_{hw}(t-T_{ii}) + R_{sw-ii} \cdot X_{sw}(t-T_{ii}) \\ & - R_{ii-pn} \cdot X_{ii,2}, \end{aligned}$$

$$\frac{dY_{ii,1}}{dt} = R_{hw-ii} \cdot [Y_{hw}(t) - Y_{hw}(t-T_{ii})] \\ + R_{sw-ii} \cdot [Y_{sw}(t) - Y_{sw}(t-T_{ii})],$$

$$\frac{dY_{ii,2}}{dt} = R_{hw-ii} \cdot Y_{hw}(t-T_{ii}) + R_{sw-ii} \cdot Y_{sw}(t-T_{ii}) \\ - R_{ii-fn} \cdot Y_{ii,2},$$

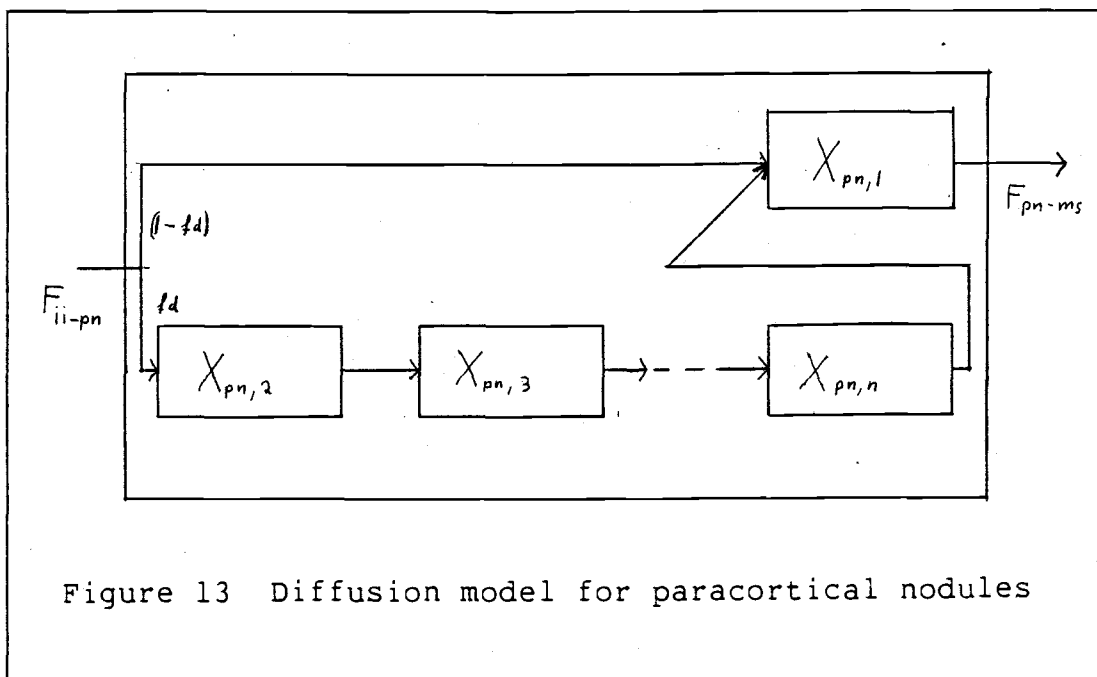
where T_{ii} will be the average transit time of lymphocytes across this region.



5. Paracortical Nodules

The next station on the route of T cells are paracortical nodules. A majority of T cells are known to remain immobilized here for several hours. Few cells however are found in the efferent lymph already 2-3 hours after having entered the node [58]. This indicates strongly that there are two parallel routes in this area, a fast one and a slow one. Following the approach we have taken so far in this model, we model the fast route

by a simple first-order compartment, while the slow route will be represented either by a chain of linear compartments or a discrete time-delay followed by a mixing compartment. A part of the incoming cells will enter the exit-compartment directly, while the majority will take the slower route through either catenary chain or discrete time-lag. Figure 13 illustrates the case where transit is modeled by a linear chain.



The equations for this case can be written as

$$\frac{dX_{pn,1}}{dt} = (1-fd) \cdot R_{ii-pn} \cdot X_{ii} + R_{pn} \cdot X_{pn,n} - R_{pn-ms} \cdot X_{pn,1}$$

$$\frac{dX_{pn,2}}{dt} = fd \cdot R_{ii-pn} \cdot X_{ii} - R_{pn} \cdot X_{pn,2}$$

$$\frac{dX_{pn,m}}{dt} = R_{pn} \cdot [X_{pn,m-1} - X_{pn,m}]$$

$$\frac{dX_{pn,n}}{dt} = R_{pn} \cdot [X_{pn,n-1} - X_{pn,n}]$$

The same region modeled by a discrete time-lag is illustrated in Figure 14. In this case the equations are

$$\frac{dX_{pn,1}}{dt} = (1-fd) \cdot R_{ii-pn} \cdot X_{ii}(t) + fd \cdot R_{ii-pn} \cdot X_{ii}(t-T_{pn}) - R_{pn-ms} \cdot X_{pn,1}$$

$$\frac{dX_{pn,2}}{dt} = fd \cdot [R_{ii-pn} \cdot X_{ii}(t) - R_{ii-pn} \cdot X_{ii}(t-T_{pn})]$$

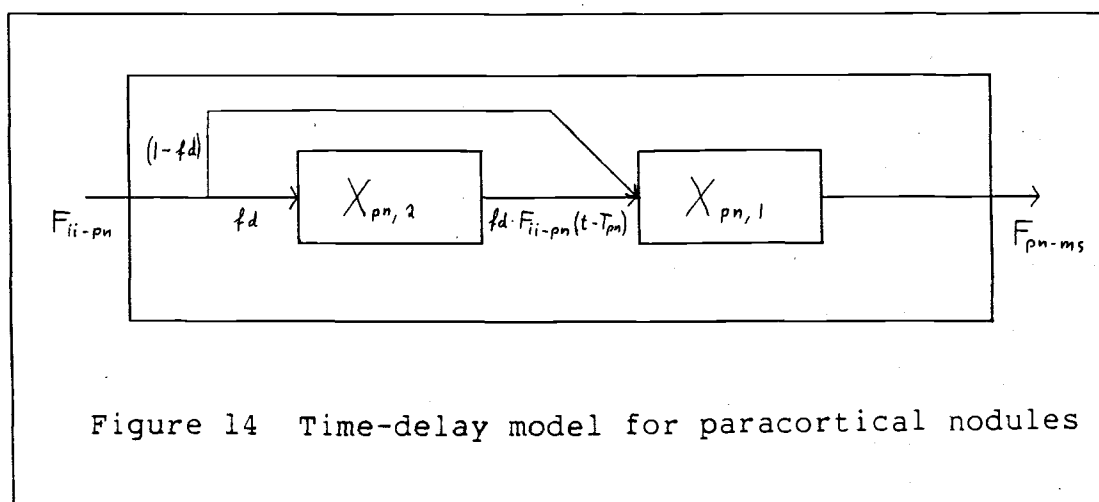


Figure 14 Time-delay model for paracortical nodules

6. Follicular nodes

B cells in follicular nodes show a very similar behavior to T cells in their respective homing region. Most of the B lymphocytes remain immobilized in this region just below the capsula for many hours before returning to medullary sinuses. However, a fast transit route must exist also, since the output of B cells begins already a few hours after injection of a tracer amount. It seems reasonable that we should model a similar

kinetic behavior with a similar model. Therefore the same approach as for paracortical nodules will be adopted for primary follicles also. An illustration for the case where transit is modeled by a catenary chain is given in Figure 15.

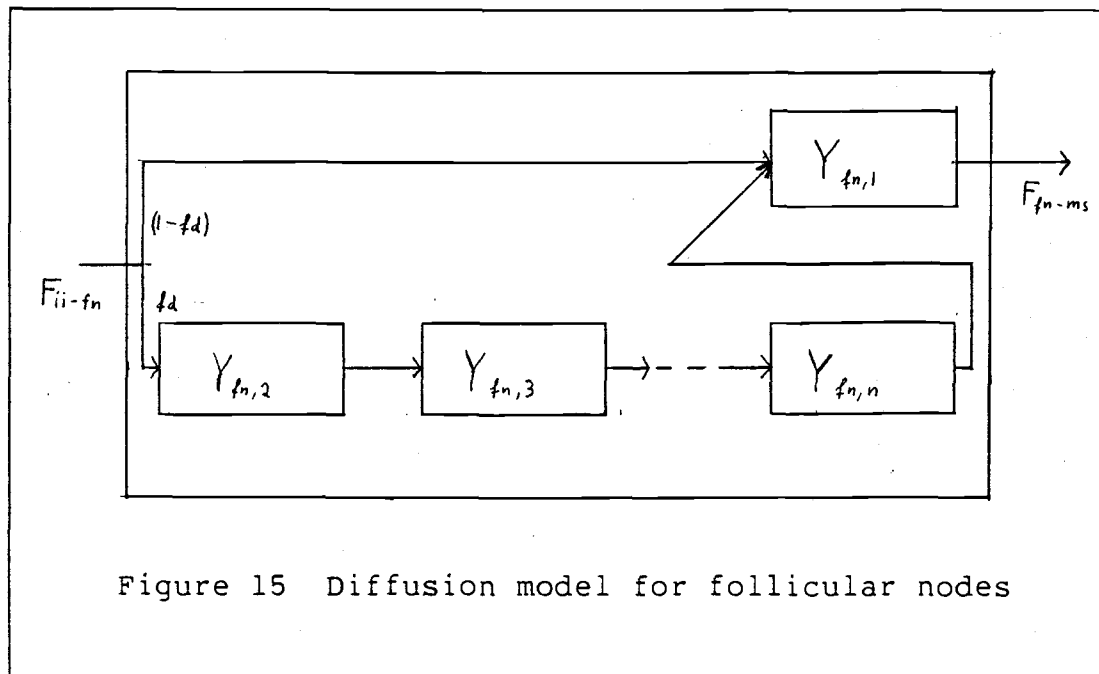


Figure 15 Diffusion model for follicular nodes

The equations for this case are

$$\frac{dY_{fn,1}}{dt} = (1-fd) \cdot R_{ii-fn} \cdot Y_{ii} + R_{fn} \cdot Y_{fn,n} - R_{fn-ms} \cdot Y_{fn,1},$$

$$\frac{dY_{fn,2}}{dt} = fd \cdot R_{ii-fn} \cdot Y_{ii} - R_{fn} \cdot Y_{fn,2},$$

$$\frac{dY_{fn,m}}{dt} = R_{fn} \cdot [Y_{fn,m-1} - Y_{fn,m}],$$

$$\frac{dY_{fn,n}}{dt} = R_{fn} \cdot [Y_{fn,n-1} - Y_{fn,n}].$$

Figure 16 illustrates the representation with a discrete time-lag. The equations for this case are

$$\frac{dY_{fn,1}}{dt} = (1-fd) \cdot R_{ii-fn} \cdot Y_{ii}(t) + fd \cdot R_{ii-fn} \cdot Y_{ii}(t-T_{fn}) - R_{fn-ms} \cdot Y_{fn,1}$$

$$\frac{dY_{fn,2}}{dt} = fd \cdot [R_{ii-fn} \cdot Y_{ii}(t) - R_{ii-fn} \cdot Y_{ii}(t-T_{fn})]$$

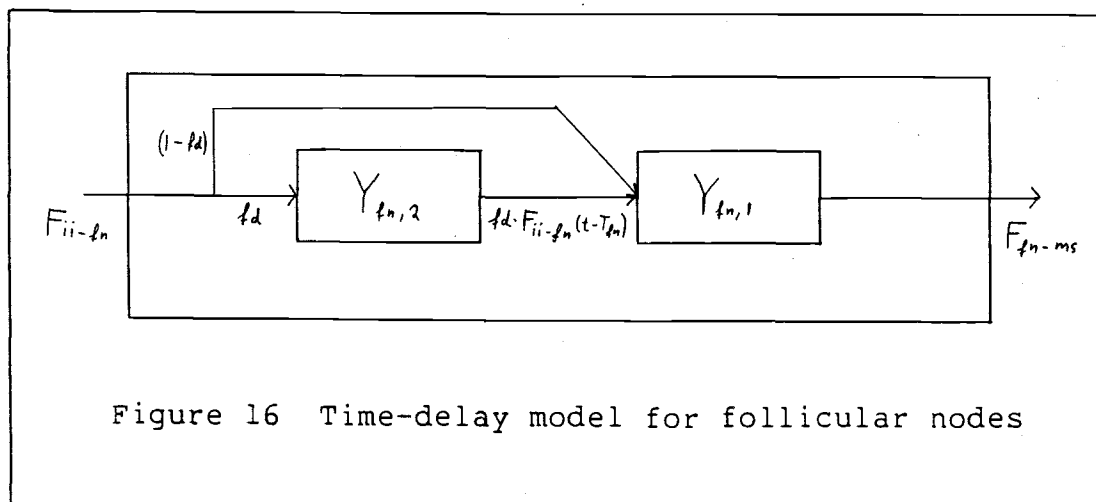


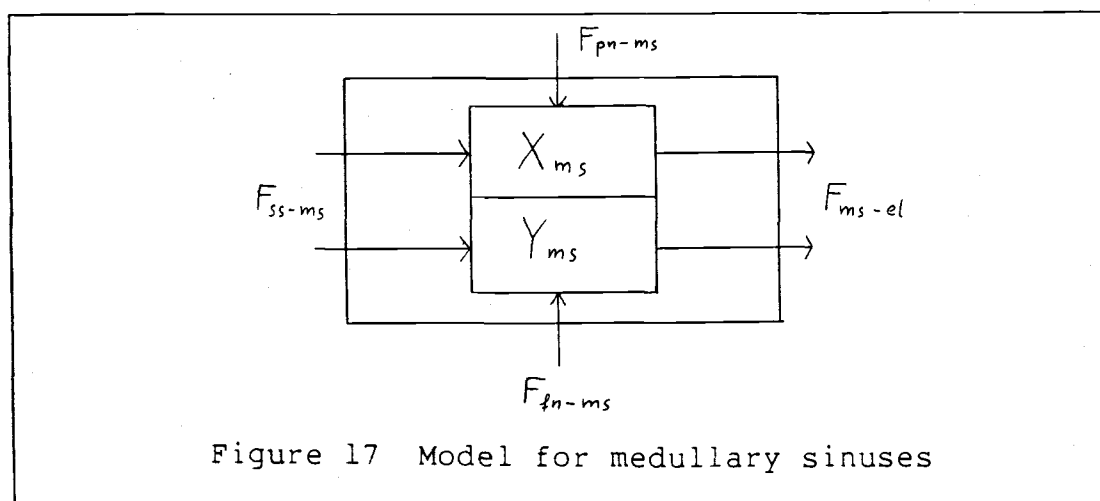
Figure 16 Time-delay model for follicular nodes

7. Medullary Sinuses

The last remaining region is the medullary sinuses, the exit station for lymphocytes in a node. B cells and T cells rejoin here and from here on share the same destiny again. Another stream joins in this compartment: Lymphocytes from afferent lymph, which have merely passed the node instead of entering it, passes through this station on their way. The output of medullary sinuses is assumed to be proportional to the lymph flow rate multiplied by the lymphocyte concentration in the compartment. An illustration is given in Figure 17 and the equations for this region are

$$\frac{dX_{ms}}{dt} = (Q_1/V_{ss}) \cdot X_{ss} + R_{pn-ms} \cdot X_{pn,1} - (Q_1/V_{ms}) \cdot X_{ms}$$

$$\frac{dY_{ms}}{dt} = (Q_1/V_{ss}) \cdot Y_{ss} + R_{fn-ms} \cdot Y_{fn,1} - (Q_1/V_{ms}) \cdot Y_{ms}$$



We can easily calculate the concentration of lymphocytes in efferent lymph as well as the B/T cell ratio from the last equations. These are measurable quantities in a tracer experiment and can therefore be used to judge the viability of the model.

RESTRICTION TO SMALLER MODEL

At this point we noted a major problem for a further analysis: While there is a reasonable good knowledge in the literature about the qualitative characteristics of lymphocyte flow through a lymphnode, good quantitative descriptions or experiments are very rare. In addition, most of the little data that is available is on T cells and is only concerned with entrance into the node from

blood. Therefore we will restrict a quantitative evaluation to the entrance of lymphocytes from blood and will neglect the second pathway from lymph.

It is due to the flexible structure of the model that this limitation to only part of the system does not have a severely damaging effect on the model. Still, neglecting the influx from lymph can only be an approximation. For peripheral nodes, this approximation can easily be justified, while it becomes questionable for central nodes. The reason is a very different concentration of lymphocytes in afferent lymph of central and peripheral lymphnodes. Peripheral lymph contains almost no lymphocytes at all, the influx into peripheral nodes from lymph will therefore be practically non-existent. Central lymph on the other hand may contain a high concentration of lymphocytes. Even though only a part of the cells coming with the afferent lymph will actually enter the node (the rest will simply stay inside the sinuses and leave again with efferent lymph), this can contribute to a considerable percentage of the total lymphocyte population.

Nevertheless the possibility that lymphocytes enter a node from lymph will be neglected in our further considerations. We have to keep in mind that this approximation might limit our results to only non-central

nodes. But again, the flexibility of the model proves to be an advantage. With more data available, this second pathway can later easily be added to the already existing model.

PARAMETER EVALUATION

The approach that was chosen leaves a whole set of parameters to be determined. Some can be derived directly from the literature. Note that some of these parameters will be different for different species. The data used for this study was obtained from the rat.

Drayson et. al. [15] give the blood flow rate to an unstimulated lymphnode of the rat as 12.9%/g of the flow to the kidney. The cardiac output of the rat was determined to be 50 ml/min [63]. 19% of the cardiac output flows to the kidneys according to the same authors. Therefore the blood flow to a 'normalized' lymphnode weighing 1g can be calculated to 1.23 ml/min for the rat.

Several authors estimate that about one out of four lymphocytes entering a node from the blood are removed by the node while the rest will leave again in the efferent blood [19,60]. This determines the rate constant R_{bl-hw} to .25.

Considering the linear chain alternative, we can estimate the number of compartments that will be needed to obtain an average transit time for each region as given in the literature. The number of cells in the n th compartment of a linear chain with rate-constant R for all compartments and an impulse input A into the first compartment will be given as

$$X_n(t) = \frac{A \cdot R \cdot t^{(n-1)} \cdot \exp(-R \cdot t)}{(n-1)!},$$

To find the value T for which this function has a maximum we set the derivative to zero and obtain the simple relation

$$n = R \cdot T + 1 .$$

A second condition for the two unknowns R and n can be found by utilizing equilibrium conditions. The rate of change of each variable in the steady-state will be zero. This determines the number of cells in compartment n to

$$X_n = N/R ,$$

where N is the number of cells entering the compartment per unit time. By adding up all X_n in the chain we obtain the total number of cells in a region.

Eliminating n results in an equation to determine the rate constant R .

$$R = \frac{N}{X_{\text{total}} - T \cdot N} .$$

The numbers on the right-hand side of this equation can

be found in the literature for the regions we are dealing with, and estimates for R and n can be calculated. However, it was found that n had to be unreasonably large to comply with the given data. We would need for example approximately 250 compartments in a chain to model paracortical nodules. Therefore the other alternative involving a discrete time delay was chosen to represent large transit-times in this model. The discrete time delay will be the average transit time of lymphocytes across a region. Estimates for these values can be found in the literature. The first labelled cells in afferent lymph are found at 1-2 hrs after injection. At about the same time the first B cells appear in follicular nodes. HEW do not contribute to a noticeable time delay. Therefore the time delay for interfollicular interstitium can be estimated to 60-120 minutes. Average transit time from blood to lymph is given as approximately 12 hours for T cells [51]. The additional time delay in the paracortex must therefore be approximately 10 hours. B cells are known to take about twice as long as do T cells to cross from blood to lymph [52], which puts the time-delay for follicular nodes to be approximately 20 hours.

The rate constants for the exchange between compartments can be estimated from equilibrium values. The following numbers can be found: About 1% of the

lymphocytes in the node are located in and around high endothelial venules, about 6.5% are in the medulla, and the overwhelming majority of 91% are found in the cortex [51]. The rate constants for the transition from HEW to paracortex and from medullary sinuses into efferent lymph can be directly calculated following the procedure given before. The constants in the paracortex itself can not be estimated that easily. Three rate constants have to be determined as well as the ratio of delayed versus non-delayed cells. Assuming that T and B cells behave in a similar manner in their respective homing regions, we will use the same rate-constant for both compartments. This assumption leaves only three constants to be determined. Only two out of these three constants are independent. After choosing two, the third constant can again be calculated from the equilibrium state. The three constants in question are: the rate constant at which cells leave the interfollicular interstitium $R_{ii-pn} = R_{ii-fn}$, the rate constant at which cells leave their respective homing region $R_{pn-ms} = R_{fn-ms}$ and the fraction of delayed cells in paracortical nodules and follicular nodes. Using our knowledge that a majority of T and B cells remain for a long time in the paracortex, while only few take the faster route, we initially chose the ratio of delayed versus non-delayed cells to 3:1. This was later adjusted to match experimental results more

closely. After fd has been chosen, the ratio of the two remaining rate constants has to be chosen. No data is available about the distribution of cells within the paracortex. Looking at the entity of the time-delay compartment with subsequent mixing, we can see that the rate constant of the mixing-compartment is responsible for the spread in the shape of the output curve. A pragmatic assumption is to choose the spread proportional to the associated time-delay. Further discussion of the estimation of parameters will follow in the next chapter.

The complete model is a system of linear differential equations with constant coefficients and with time-delays. No feedback is included, that is each compartment is influenced only by its input and its state. State in this sense includes the infinite state space of time-delay compartments. In contrast to ordinary differential equations which can be evaluated at an instantaneous time t , this system is dependent on the previous history during a finite time T . The model can be divided into two parts for T and B cells respectively. These parts are identical except for a longer time-delay in the B cell equations. A closed-form solution can not readily be obtained due to the nature of the time-delays. However, an examination of the stability of the model was performed. The equation for the time-delay compartments can be written in the form

$$\frac{dX(t)}{dt} = U(t) - U(t-T),$$

Where $X(t)$ is the number of cells in the compartment and $U(t)$ is its input at time t . T is a finite, constant and positive time-delay. This equation can easily be solved by integration and it can be seen from the solution that this system is bounded for any input-function U that is bounded over all time-intervals T .

$$\int_{t=0}^{t+T} U(t)dt < K < \infty \quad \text{for all } t > -T .$$

The equations for the time-delay compartments can be decoupled from the rest of the system without affecting the structure of the remaining equations. The remaining part of the system is a set of linear differential equations with time-delays which can be examined by finding the roots of the characteristic equation. This system can be written in the form

$$\frac{dX}{dt} = A \cdot X(t) + B \cdot X(t-T_1) + C \cdot X(t-T_2) + D \cdot U, \quad (1)$$

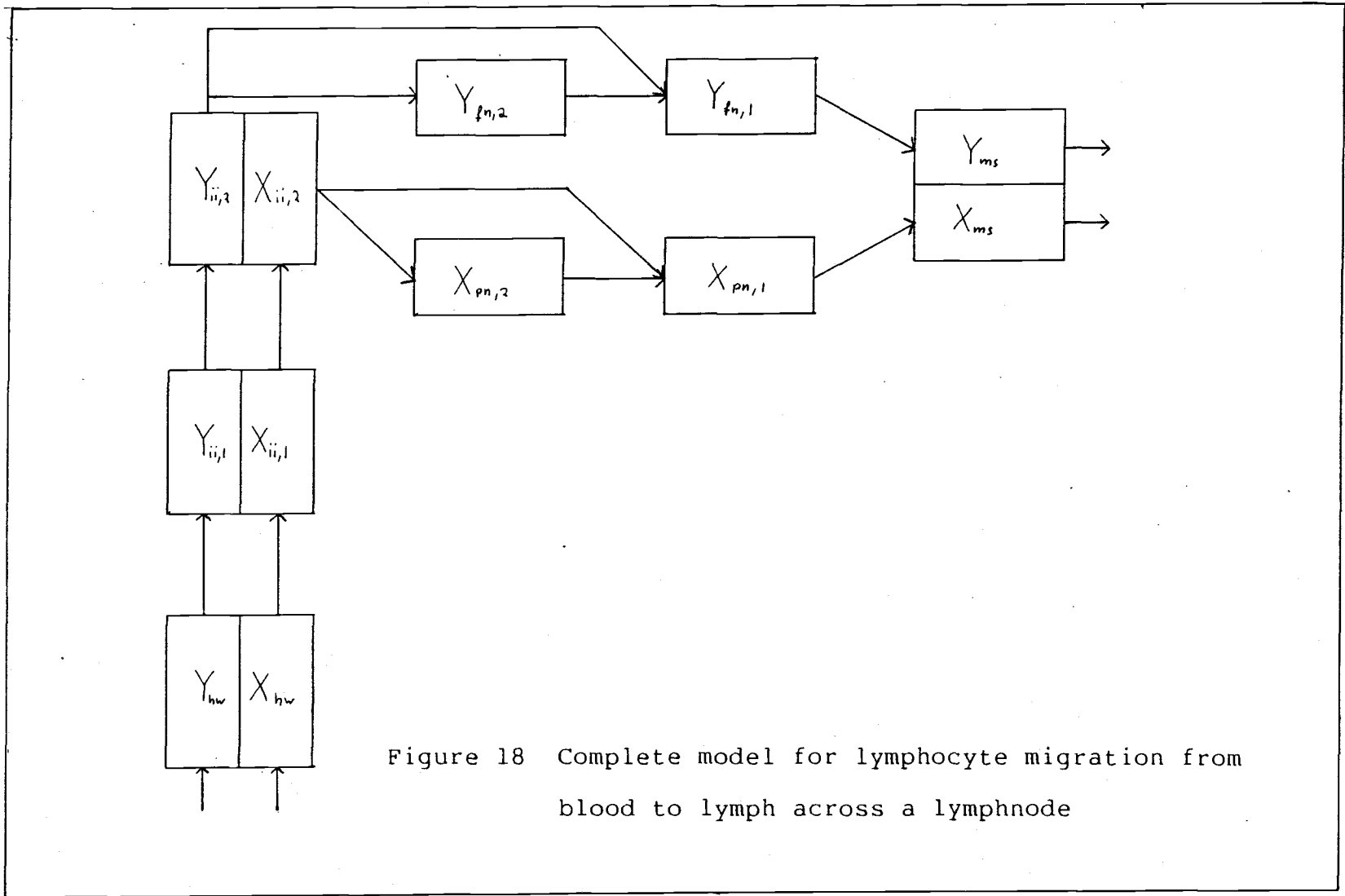
where X is the vector of state variables, U is the input-vector and A, B, C and D are constant matrices. The characteristic equation for this system is then given by [16] to

$$\det[\lambda \cdot I - A - B \cdot \exp(-\lambda \cdot T_1) - C \cdot \exp(-\lambda \cdot T_2)] = 0 . \quad (2)$$

A system of linear differential equations with constant coefficients and time-delays of form (1) is stable if the

roots of the characteristic equation all have negative real parts and if the input to the system is bounded. The roots of the characteristic equation were found to be the negative rate constants. It follows that the system is stable if all the rate constants are positive.

The model also is deterministic, that is it does not take into consideration any noise in system or measurements. An illustration for the complete model is given in Figure 18.



The complete model is listed below

$$\frac{dX_{hw}}{dt} = R_{bl-hw} Q_{bl} C_{bt} - R_{hw-ii} X_{hw}$$

$$\frac{dY_{hw}}{dt} = R_{bl-hw} Q_{bl} C_{bb} - R_{hw-ii} Y_{hw}$$

$$\frac{dX_{ii,1}}{dt} = R_{hw-ii} [X_{hw}(t) - X_{hw}(t-T_{ii})]$$

$$\frac{dX_{ii,2}}{dt} = R_{hw-ii} X_{hw}(t-T_{ii}) - R_{ii-pn} X_{ii,2}$$

$$\frac{dY_{ii,1}}{dt} = R_{hw-ii} [Y_{hw}(t) - Y_{hw}(t-T_{ii})]$$

$$\frac{dY_{ii,2}}{dt} = R_{hw-ii} Y_{hw}(t-T_{ii}) - R_{ii-fn} Y_{ii,2}$$

$$\begin{aligned} \frac{dX_{pn,1}}{dt} = & (1-fd) R_{ii-pn} X_{ii,2}(t) + fd R_{ii-pn} X_{ii,2}(t-T_{pn}) \\ & - R_{pn-ms} X_{pn,1} \end{aligned}$$

$$\frac{dX_{pn,2}}{dt} = fd [R_{ii-pn} X_{ii,2}(t) - R_{ii-pn} X_{ii,2}(t-T_{pn})]$$

$$\begin{aligned} \frac{dY_{fn,1}}{dt} = & (1-fd) R_{ii-fn} Y_{ii,2}(t) + fd R_{ii-fn} Y_{ii,2}(t-T_{fn}) \\ & - R_{fn-ms} Y_{fn,1} \end{aligned}$$

$$\frac{dY_{fn,2}}{dt} = fd [R_{ii-fn} Y_{ii,2}(t) - R_{ii-fn} Y_{ii,2}(t-T_{fn})]$$

$$\frac{dX_{ms}}{dt} = R_{pn-ms} X_{pn,1} - R_{ms-el} X_{ms}$$

$$\frac{dY_{ms}}{dt} = R_{fn-ms} Y_{fn,1} - R_{ms-el} Y_{ms}$$

TABLE 1

List of variables

X_{hw}	T cell population in HEW
Y_{hw}	B cell population in HEW
$X_{ii,1}$	T cell population in time-delay compartment of interfollicular interstitium
$X_{ii,2}$	T cell population in mixing compartment of interfollicular interstitium
$Y_{ii,1}$	B cell population in time-delay compartment of interfollicular interstitium
$Y_{ii,2}$	B cell population in mixing compartment of interfollicular interstitium
$X_{pn,1}$	T cell population in mixing compartment of paracortical nodules
$X_{pn,2}$	T cell population in time-delay compartment of paracortical nodules
$Y_{fn,1}$	B cell population in mixing compartment of follicular nodes
$Y_{fn,2}$	B cell population in time-delay compartment of follicular nodes
X_{ms}	T cell population of medullary sinuses
Y_{ms}	B cell population of medullary sinuses

TABLE 2

List of constants

Q_{bl}	Blood flow rate
C_{blt}	Concentration of T cells in blood
C_{blb}	Concentration of B cells in blood
R_{bl-hw}	Rate constant from blood to HEW
R_{hw-ii}	Rate constant from HEW to interfollicular interstitium
R_{ii-pn}	Rate constant from interfollicular interstitium to paracortical nodules
R_{ii-fn}	Rate constant from interfollicular interstitium to follicular nodes
R_{pn-ms}	Rate constant from paracortical nodules to medullary sinuses
R_{fn-ms}	Rate constant from follicular nodes to medullary sinuses
R_{ms-el}	Rate constant from medullary sinuses to efferent lymph
fd	Fraction of delayed cells in paracortical nodules and follicular nodes

V. SIMULATION

COMPUTER PROGRAM

FORTRAN 77 was used to run the simulation program on an HP1000 computer. A fourth order Runge-Kutta algorithm was used for the integration. The time constants in the model range from 0.0085 to .125. They differ only by a factor 15 which shows that we are not dealing with a stiff system. No special precautions have to be considered for the integration and a fourth-order Runge-Kutta method will give good accuracy.

The fastest time response is given by the largest rate constant. A value of .125 was determined for R_{hw-ii} , the rate constant between HEW and interfollicular interstitium. This puts the fastest time response to $(1/R_{hw-ii})$ or 8 minutes. With a step-function as input the maximum error will occur during the first integration step. For a step-size of 1 minute, the maximal error was calculated to be 1.05%. The step-size was therefore chosen to 1 minute as a good compromise between accuracy and computing time.

To test the model, an experiment by Smith and Ford [58] on rats was simulated. In this experiment, thoracic duct cells of a donor rat were radioactively labeled and

passed from blood to lymph in an intermediate rat. These passaged cells were injected into a series of final recipients and their concentration in several organs as well as in blood was measured at different time intervals. Using the measured blood concentration as an input to the model, a simulation will produce the total number of lymphocytes in a node as one output. The result from the simulation can then be compared to data from the experiment. Smith and Ford examined several different lymphnodes in their experiment. We will only use the data from superficial cervical, deep cervical and left popliteal node as a reference for the model. The blood flow to coeliac nodes comes from the liver as shown in Figure 5 and can therefore not be assumed to be the same as for other nodes. A similar argument holds for mesenteric nodes, whose input is partially derived from gut. The right popliteal node was stimulated with antigen and will therefore also not be used for comparison.

The B cell fraction in the injected substance is estimated to be only 10% [59], which is substantially lower than the usual 30%. This may be due to the passage through an intermediate rat. Collection of thoracic duct lymph from this intermediate rat produces a high proportion of T cells due to their more rapid transit through lymphnodes. Concentration of T and B cells in

blood was assumed proportional to total lymphocyte concentration in blood with a proportionality factor 0.9 for T cells and 0.1 for B cells.

PARAMETER ADJUSTMENT

To compare the simulation with experimental results, the total number of lymphocytes in the node was calculated by adding up the numbers of all single compartments. The result and the comparison to experimental data is shown in Figure 19.

Several parameters were adjusted in order to better match experimental results. While the rate constants for HEW and medullary sinuses are reasonably well determined by steady-state conditions the same is not true for the parameters in the cortex. Even after simplifying assumptions have been made in the last chapter there still remain five parameters to be identified. These are specifically T_{ii} , T_{pn} and T_{fn} - the discrete time-delays in interfollicular interstitium, paracortical nodules and follicular nodes, f_d - the fraction of delayed cells, and R_{ii-pn}/R_{pn-ms} - the ratio of the two remaining rate constants.

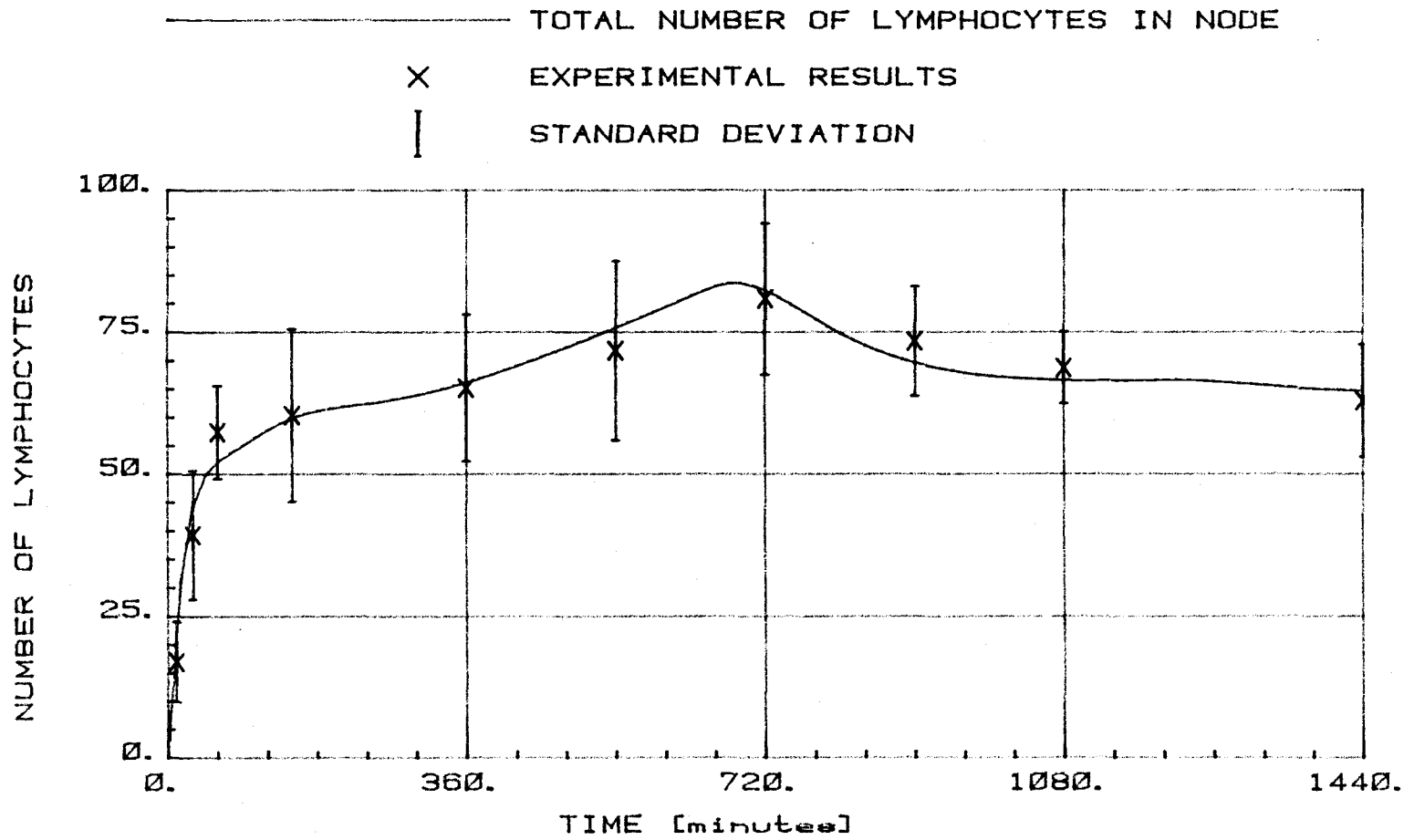


Figure 19 Comparison of literature data and simulation results

After varying these constants independently it was noted that a change of the ratio of the rate constants did have little effect on the total number of cells in the node. Data from this experiment will therefore not allow a better estimation of this constant.

A similar argument holds for the average transit-time in follicular nodes. Due to the extremely small fraction of B cells in this experiment a variation of this constant shows little effect on the total number of cells in the node. The fraction of B cells in the experiment is too small to be reasonably well reflected in measurements. In absence of better data we will continue estimating T_{fn} to twice the time-delay of T cells.

A more methodic parameter estimation could be performed for the remaining three parameters. Using least square estimation, the sum of the square of the error was calculated as a quality factor.

$$Q = \sum_{j=1}^m (Y - \hat{Y})^2.$$

Minimizing this sum with respect to T_{ii}, T_{pn} and fd will result in optimal values for all three parameters. Estimates for all three parameters were given in the

previous chapter. By varying all parameters in the vicinity of these previous estimates a minimum was found for the quality factor. The optimal values for the parameters were found to be 90 minutes for the time-delay in interfollicular interstitium, 9 hours for the delay-time in paracortical nodules and 0.7 for the fraction of cells which take the slower route in paracortical nodules and follicular nodes. The determination of T_{ii} according to this method seems rather questionable since the sensitivity of the quality factor on variations in T_{ii} was very low.

SIMULATION RESULTS

With all parameter values determined, results of the simulation are shown in Figure 20. We note a steep rise in lymphocyte population during the first sixty minutes after injection, corresponding to the exponential fall in blood. When the concentration in blood has reached equilibrium, the rise slows down significantly, but is maintained until twelve hours after injection. Then a slow descent begins to continue until the steady state is reached at about 24 hours after injection.

The simulated result matches almost perfectly the given data points of the experiment. This shows that the model is able to reproduce the dynamic behavior of a lymphnode for the particular input of this experiment.

- # OF CELLS IN TOTAL NODE
- # OF CELLS IN INTERFOLICULAR INTERSTITIUM
- - - - - # OF CELLS IN PARACORTICAL NODULES
- - - - - # OF CELLS IN PARACORTEX

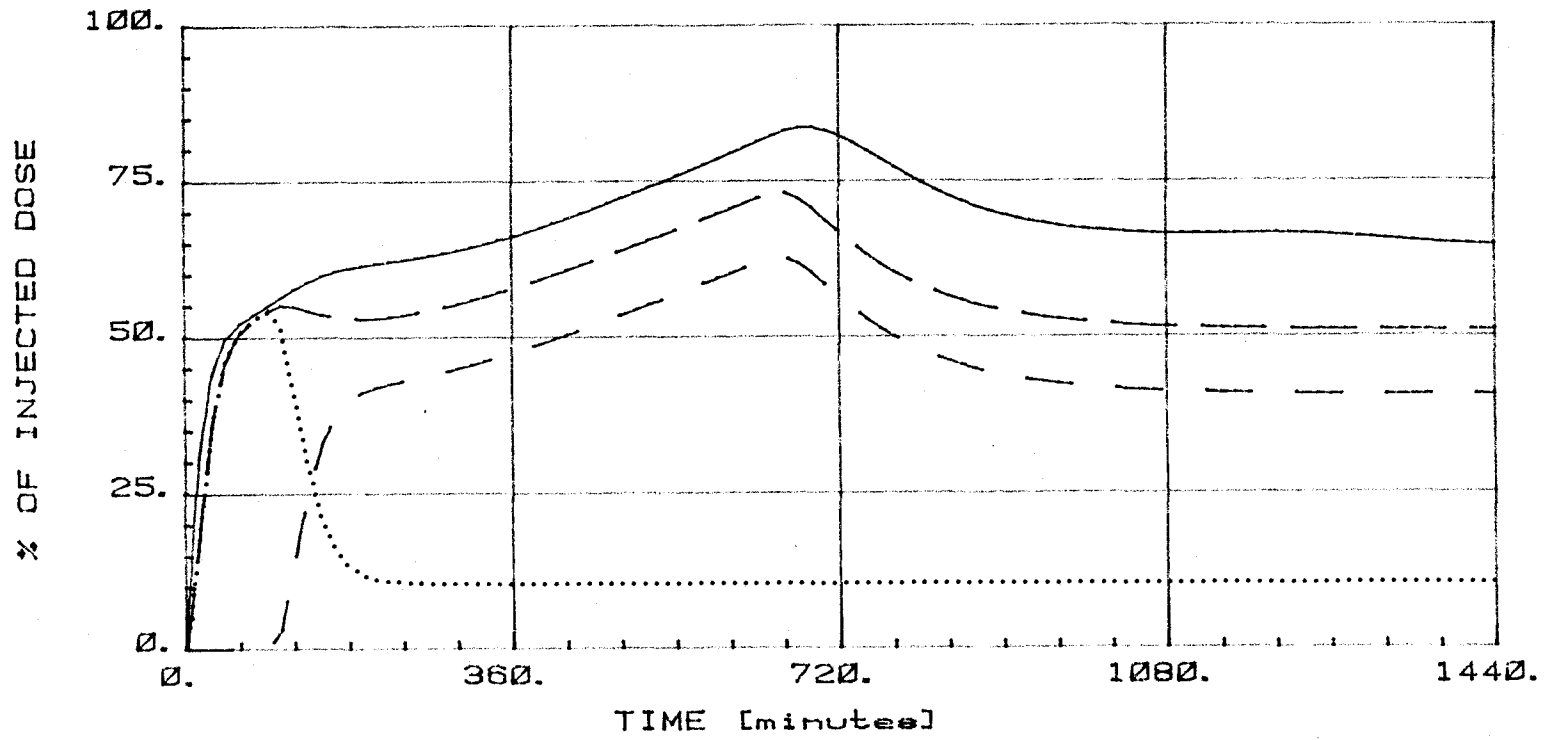


Figure 20a Simulation results I for laboratory experiment

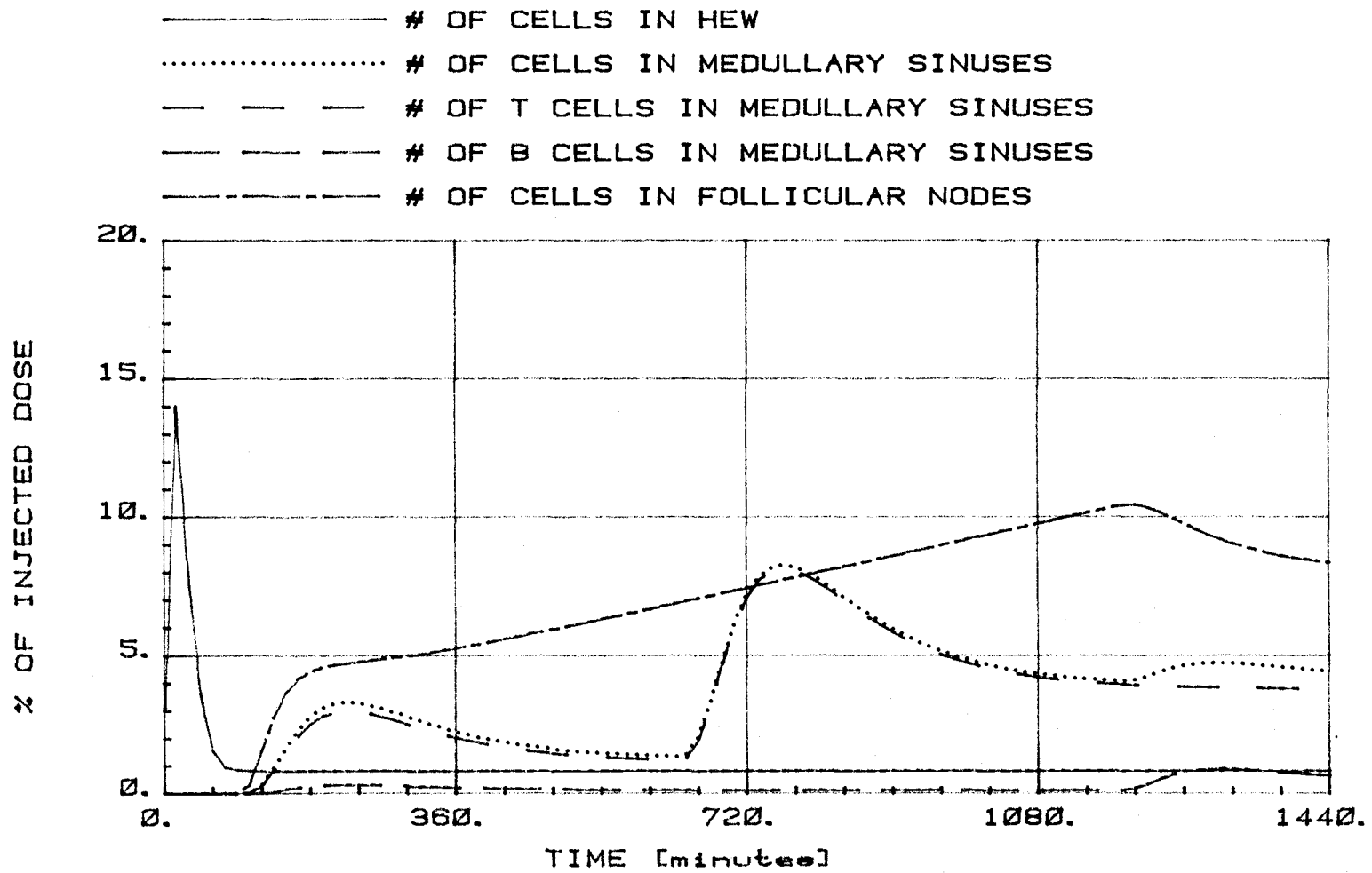


Figure 20b Simulation results II for laboratory experiment

The model also predicts the distribution of lymphocytes within the node during this experiment.

The number of lymphocytes in HEW rises sharply in the beginning to reach a peak only 20 minutes after injection. Then a steep decline begins to end in an equilibrium value of about 1% after only 2 hours. This result is consistent with qualitative descriptions [52,58]. A vast majority of cells reside in the paracortex, therefore we expect here a similar behavior as for the total node. The number of cells in the paracortex is the sum of the populations of interfollicular interstitium and paracortical nodules. The peak here is reached slightly earlier as for the entire node, at about 10 hours after injection. Looking into the subareas of the cortex, we find for interfollicular interstitium a sharp rise in the beginning followed by a peak at 90 minutes and an exponential decline to the steady state value which is reached about 3 hours after injection. The uptake in paracortical nodules and follicular nodes does not begin until 90 minutes after injection. Both regions display a steep rise in cell population for about one hour, followed by a distinctive shoulder and a much slower rise. They reach their maxima at 11 and 20 hours respectively.

Medullary sinuses finally show a small population increase beginning at 2 hours after injection with a first peak at 4 hours, followed by a second larger rise with its peak about twelve hours after injection. This second rise is due to the release of cells that were stored in paracortical nodes.

Looking at T and B cells separately, we note that there are very few B cells in medullary sinuses during the first 15 hours after injection. Since the number of cells leaving the node via efferent lymph is proportional to their number in medullary sinuses, we can conclude that the lymphocyte population in efferent lymph during the first 15 hours after injection consists almost exclusively of T cells. The obtained results are consistent with qualitative descriptions of lymphocyte-kinetics in lymphnodes [29,52]

To find the dependency of the model on the input, the simulation was performed for several different input functions. A step-function was applied at $t=0$ with the input rising from 0 to .3, which is the equilibrium value of the first simulation. The results are shown in Figure 21. A slow and almost linear increase of the total number of cells in the node is noted during the first twelve hours, due to the build up of T cells in the paracortex.

- # OF CELLS IN TOTAL NODE
- # OF CELLS IN INTERFOLICULAR INTERSTITIUM
- - - - - # OF CELLS IN PARACORTICAL NODULES
- - - - - # OF CELLS IN PARACORTEX

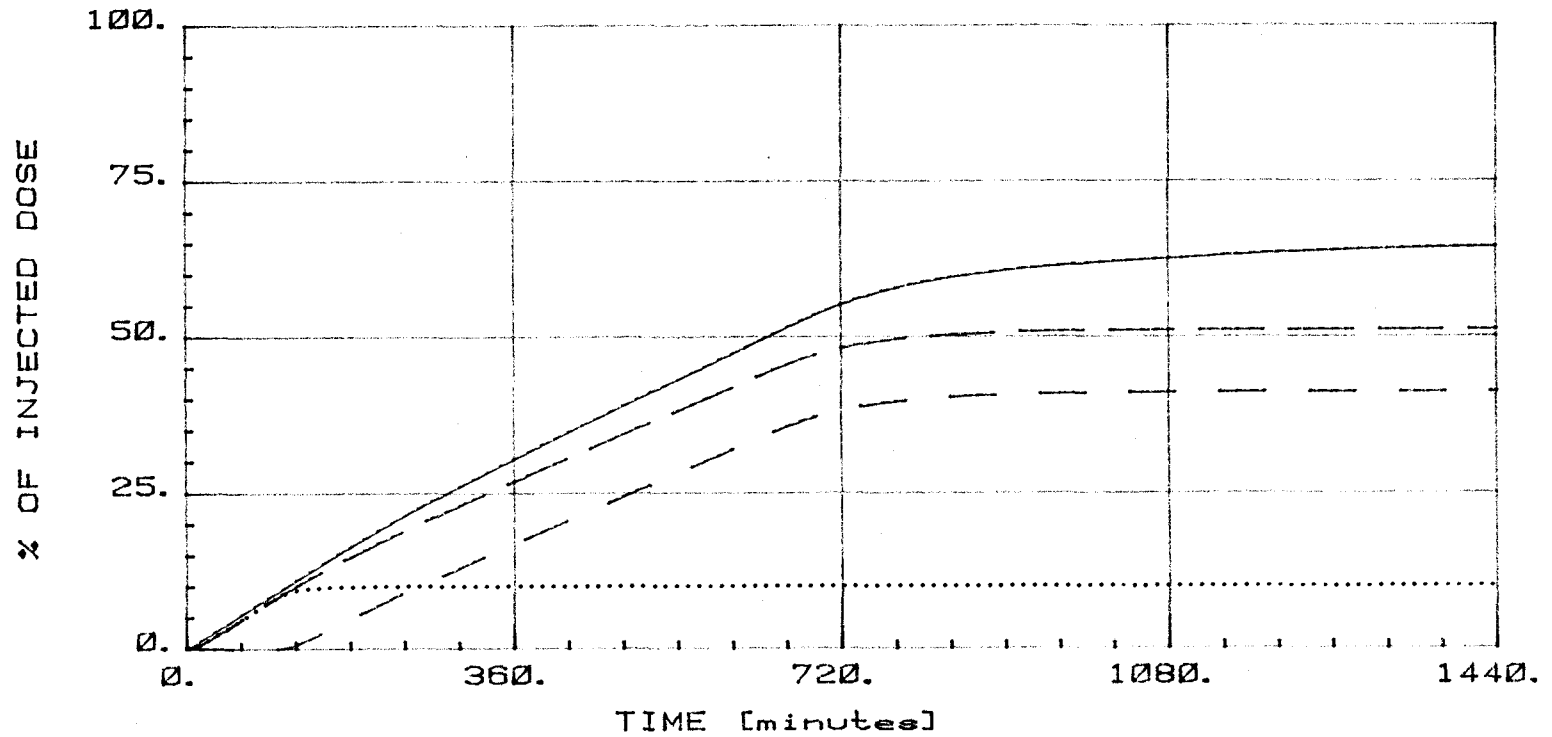


Figure 21a Simulation results I for step-input

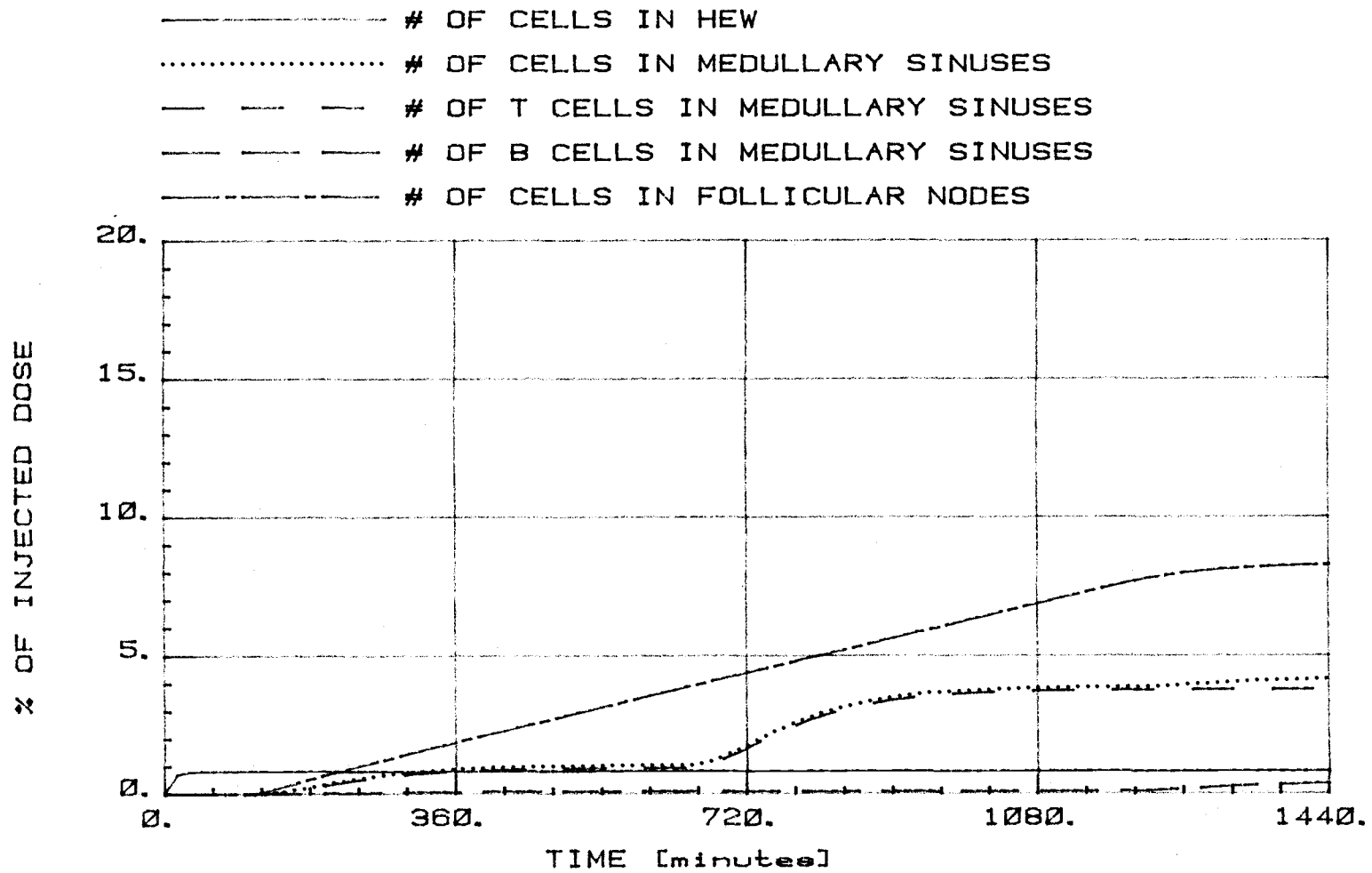


Figure 21b Simulation results II for step-input

A considerably smaller increase during the next twelve hours is caused by a still increasing number of B cells, while T cells have reached equilibrium already. Afferent lymph during the first twenty hours consists almost solely out of T cells.

The large storage effect of a node can be seen in Figure 22. The simulation began at equilibrium, but the input was cut off at $t = 120$ minutes. It is noted that T cells leave the node much more rapidly than B cells do. An interesting effect is that the number of cells in the efferent lymph does not considerably decrease during the first eleven hours after cutoff.

Figure 23 shows how a short bolus proceeds through the node. The input was set to a constant level for ten minutes and switched back to zero afterwards. The initial states were again all set to zero. Some interesting effects are an extremely long almost constant population in follicular nodes and three distinctive peaks in the cell output of the node. A first peak consists out of both T and B cells while the second and largest peak is solely due to T cells being released from paracortical nodes. The third and smallest peak follows 21 hours after the bolus has been injected and consists out of B cells.

_____ # OF CELLS IN TOTAL NODE
 # OF CELLS IN INTERFOLICULAR INTERSTITIUM
 - - - - - # OF CELLS IN PARACORTICAL NODULES
 - - - - - # OF CELLS IN PARACORTEX

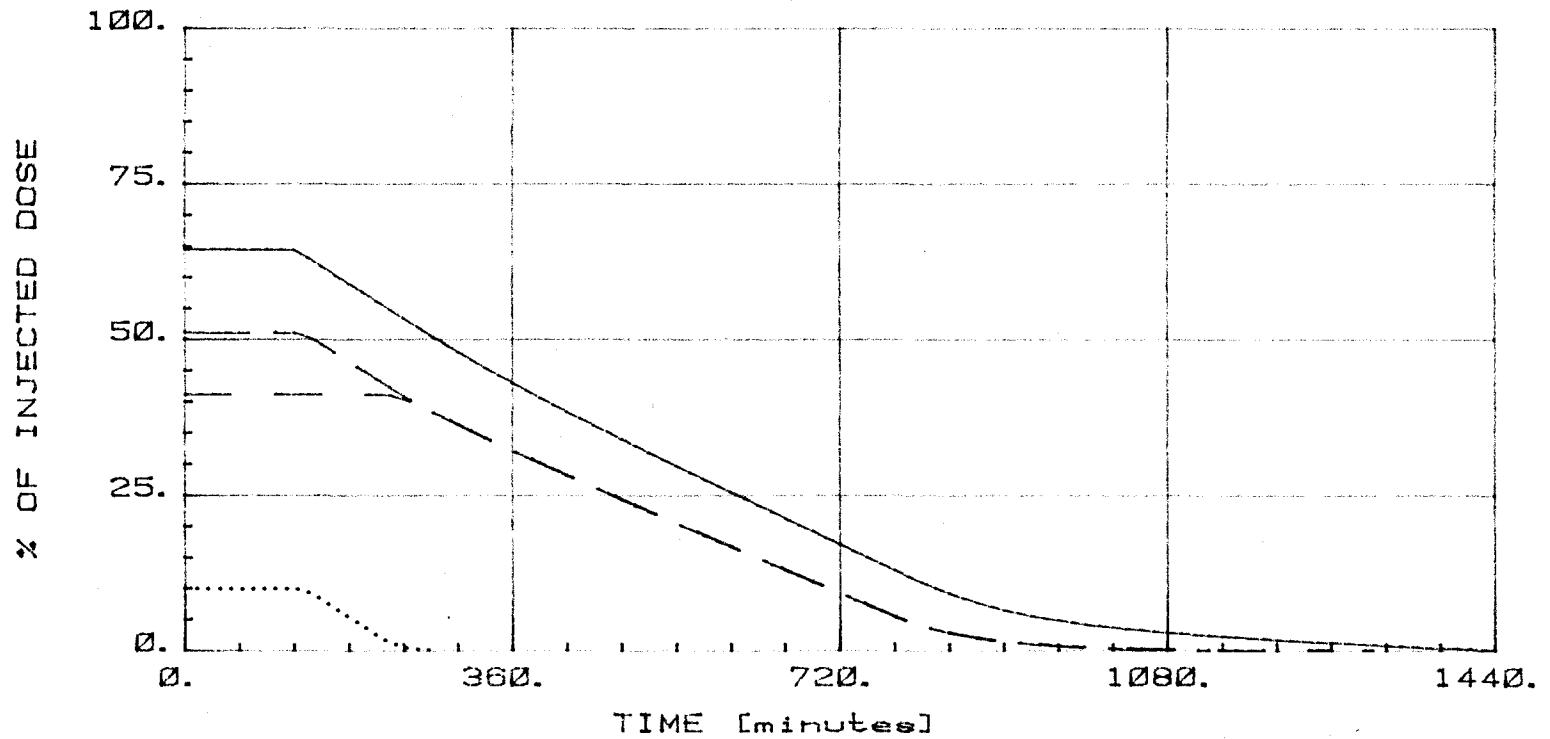


Figure 22a Simulation results I for input set to 0 at 120 minutes

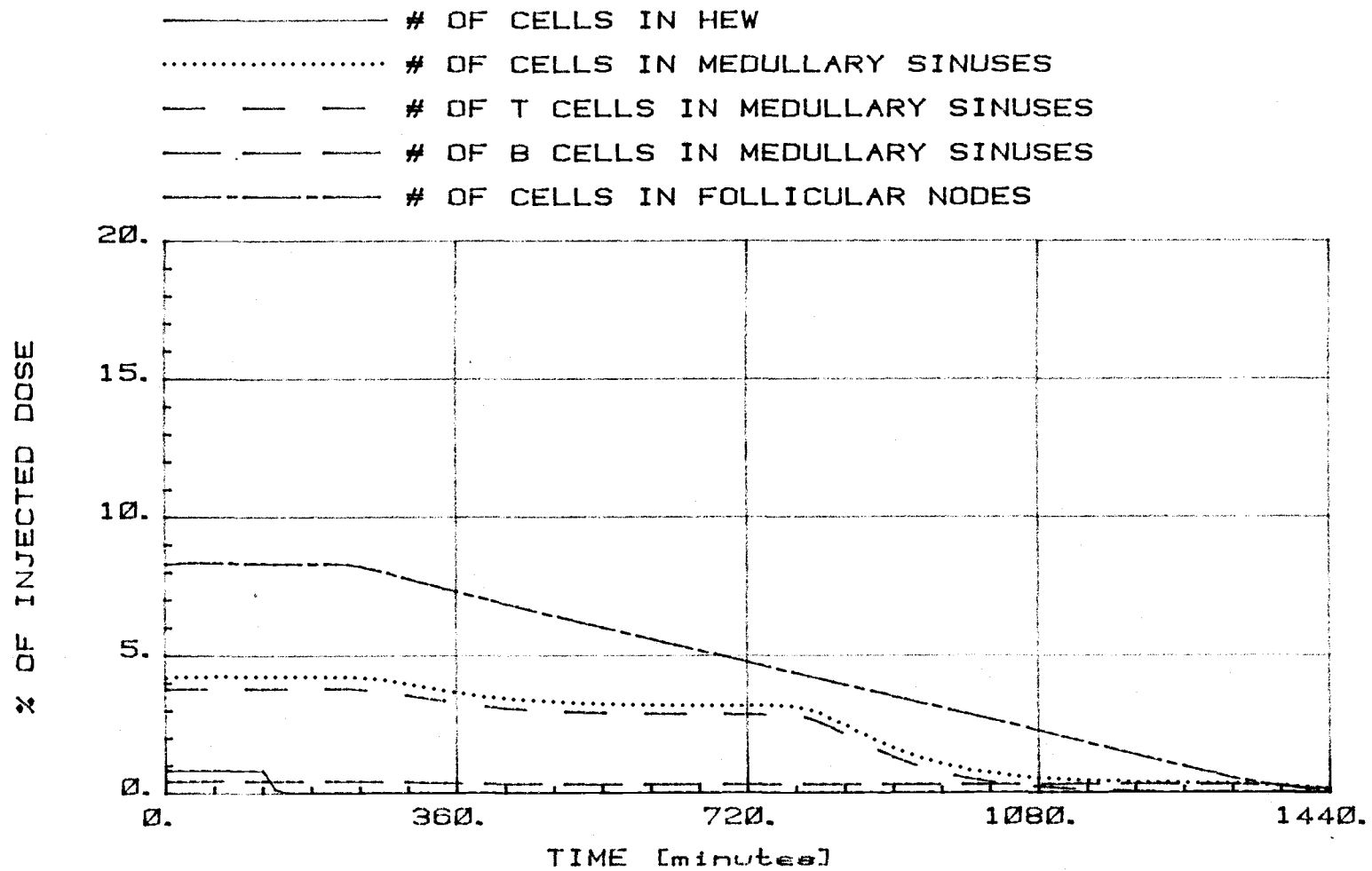


Figure 22b Simulation results II for input set to 0 at 120 minutes

----- # OF CELLS IN TOTAL NODE
 # OF CELLS IN INTERFOLICULAR INTERSTITIUM
 - - - - - # OF CELLS IN PARACORTICAL NODULES
 — — — — # OF CELLS IN PARACORTEX

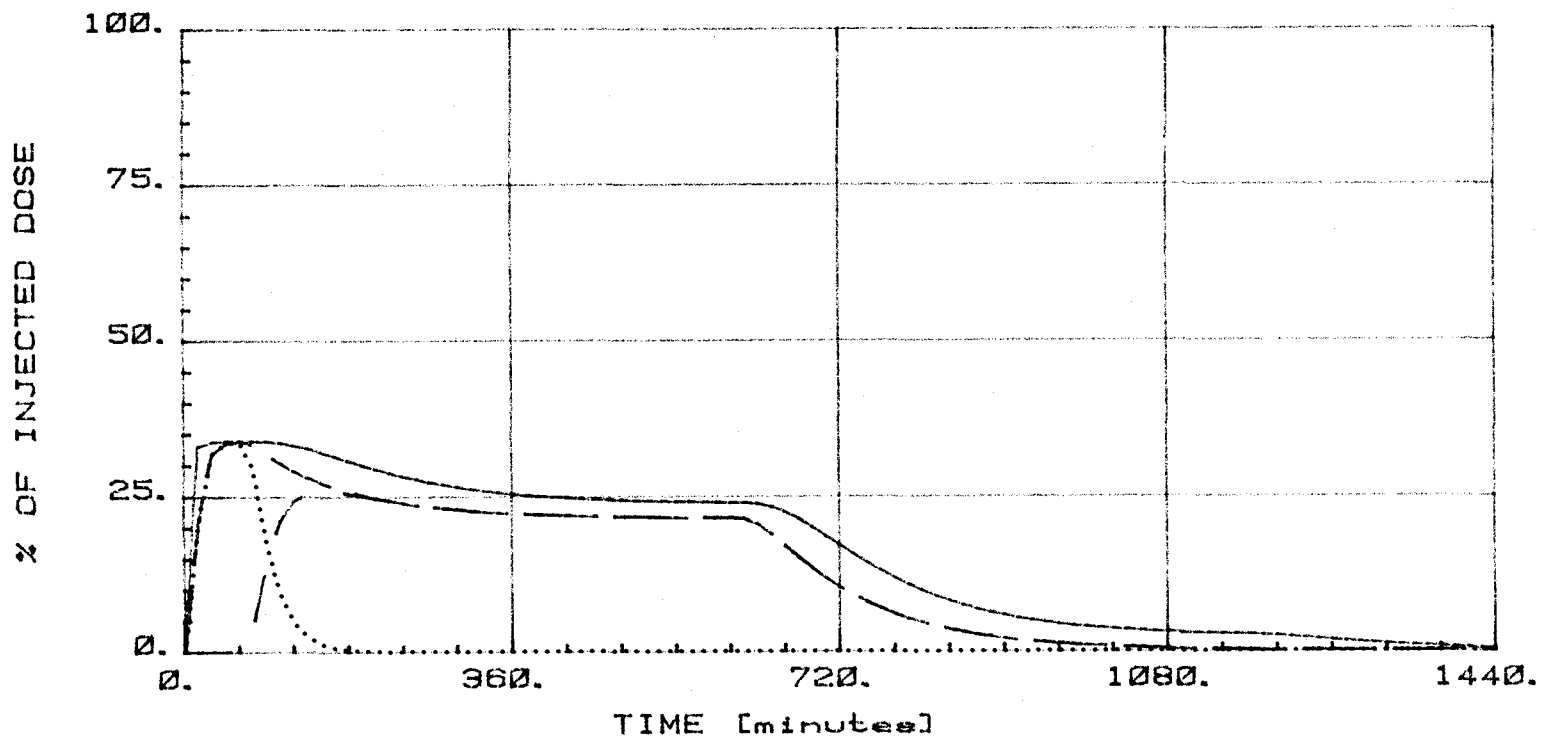


Figure 23a Simulation results I for bolus input

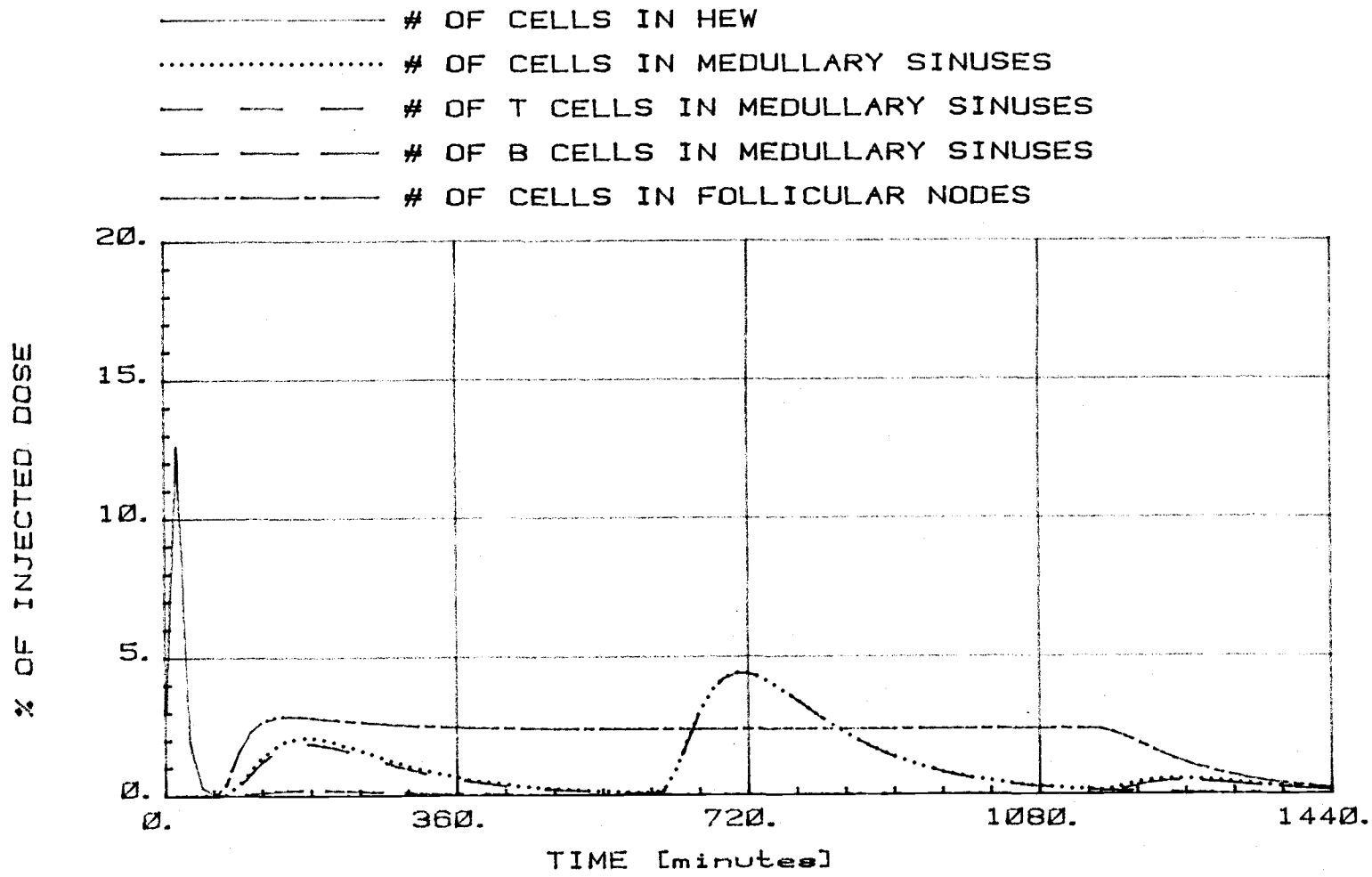


Figure 23b Simulation results II for bolus input

Two more simulations were performed to study the effects of input variation on the cell population of a node. Figure 24 shows results for the same exponential function that was used to model blood concentration of Smith and Ford's experiment, but instead of reaching a steady value at 60 minutes as before, the exponential function is now continued down to zero. A noticeable difference is observed from the first simulation. Figure 25 shows the effects of an input that decreases linearly instead of exponentially during the first sixty minutes and is switched to the same steady-state value afterwards. Note the different scale in Figure 25a.

- # OF CELLS IN TOTAL NODE
- # OF CELLS IN INTERFOLICULAR INTERSTITIUM
- - - - # OF CELLS IN PARACORTICAL NODULES
- # OF CELLS IN PARACORTEX

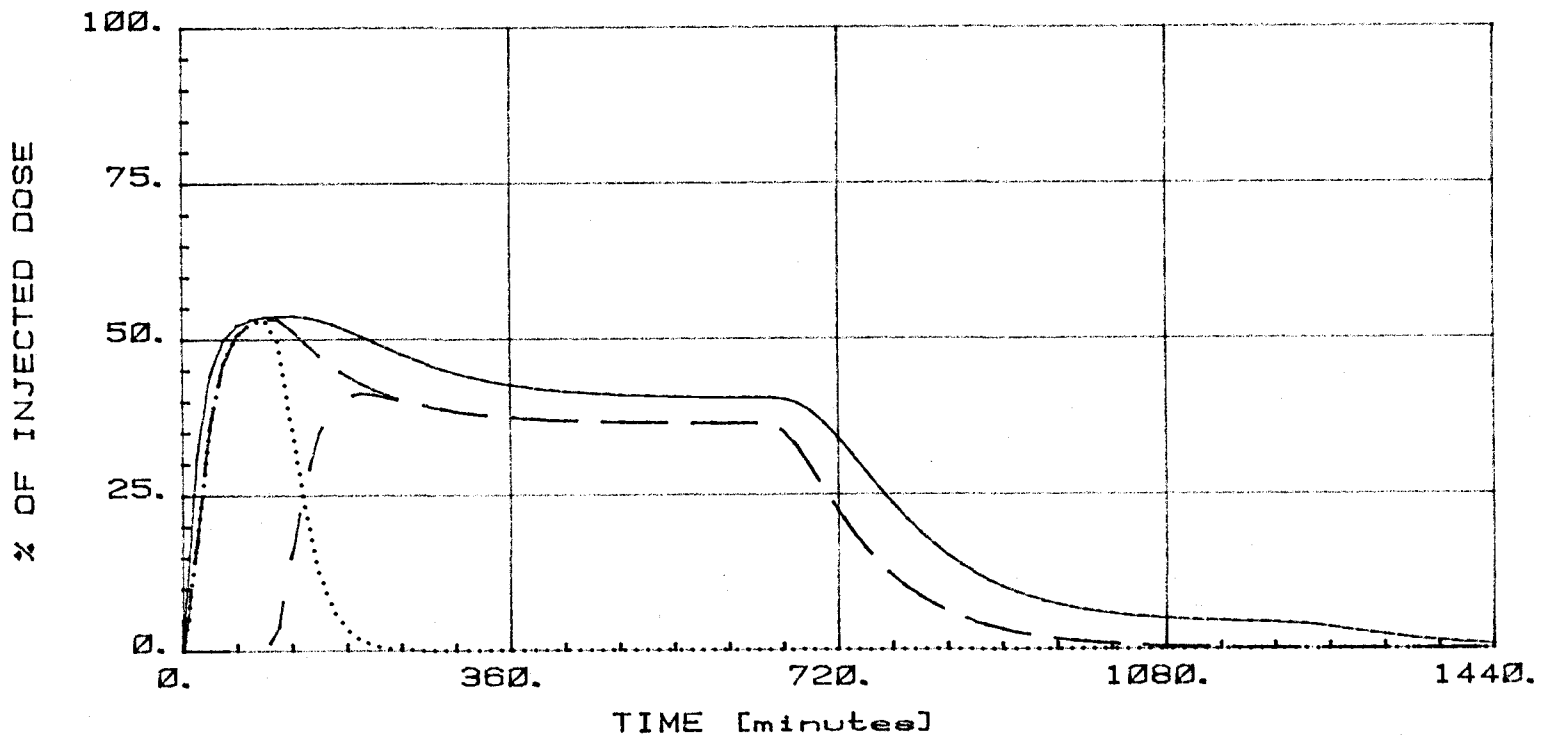


Figure 24a Simulation results I for exponential input

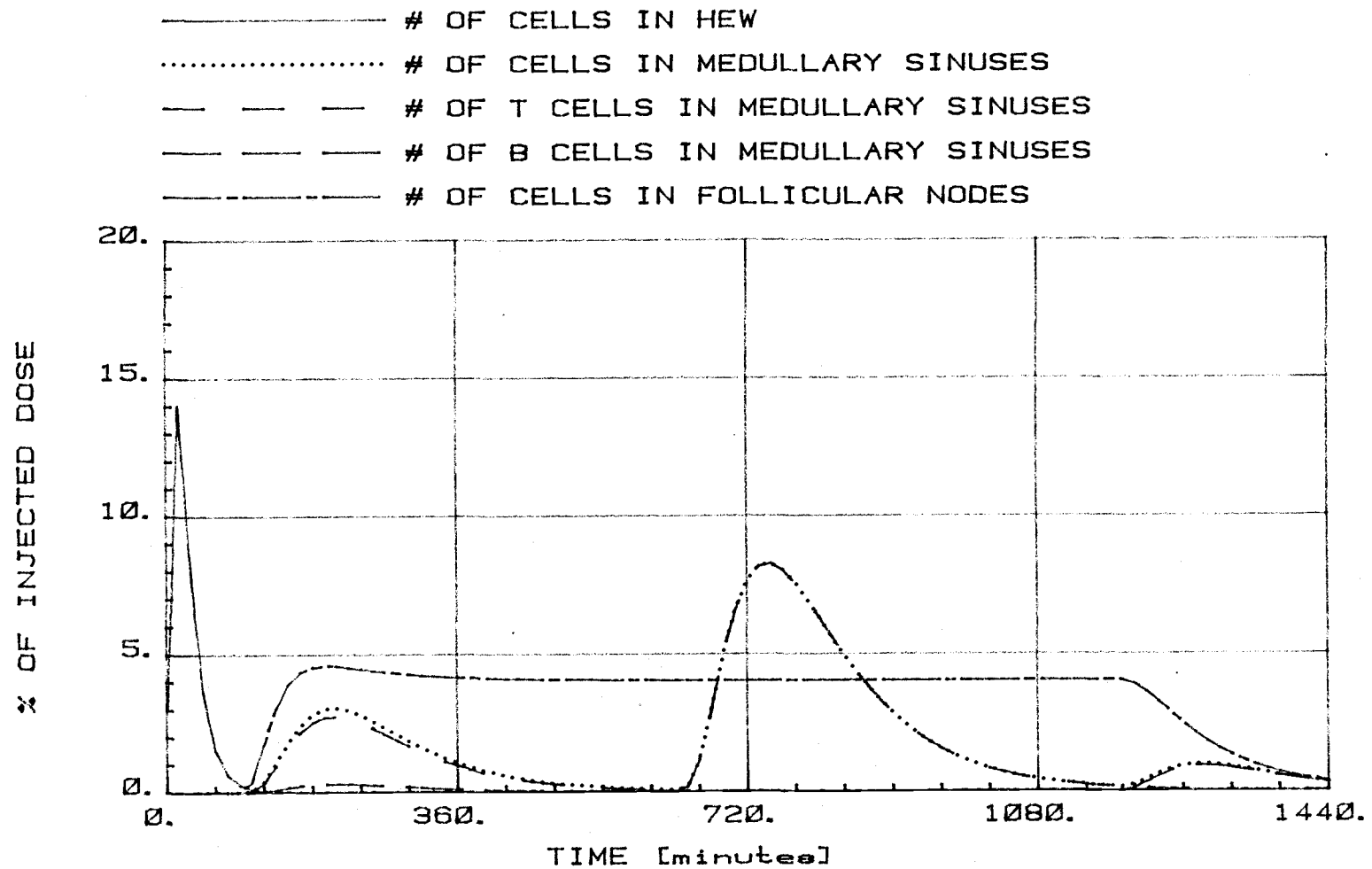


Figure 24b Simulation results II for exponential input

- # OF CELLS IN TOTAL NODE
- # OF CELLS IN INTERFOLICULAR INTERSTITIUM
- - - - # OF CELLS IN PARACORTICAL NODULES
- - - - # OF CELLS IN PARACORTEX

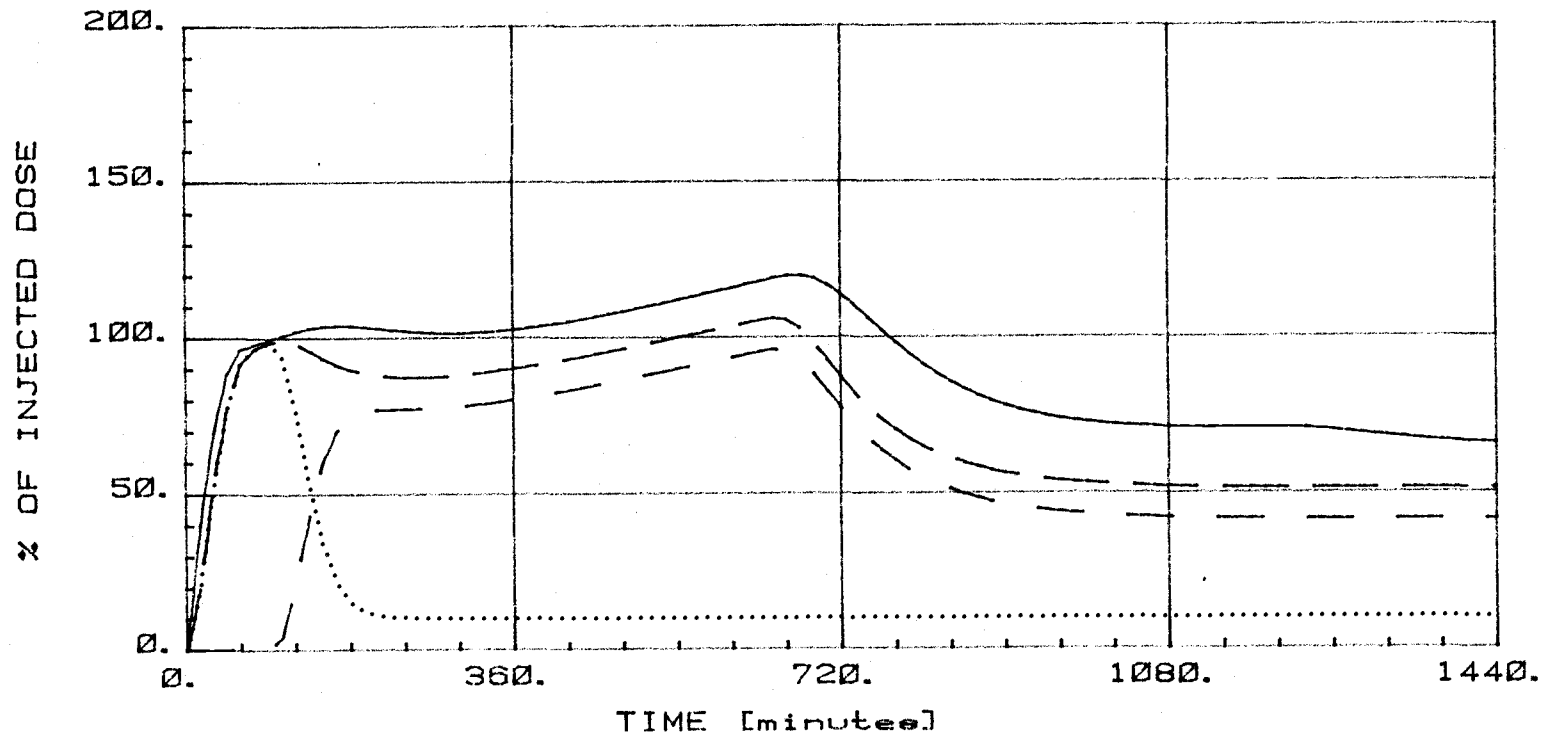


Figure 25a Simulation results I for linear decreasing input with constant limit value

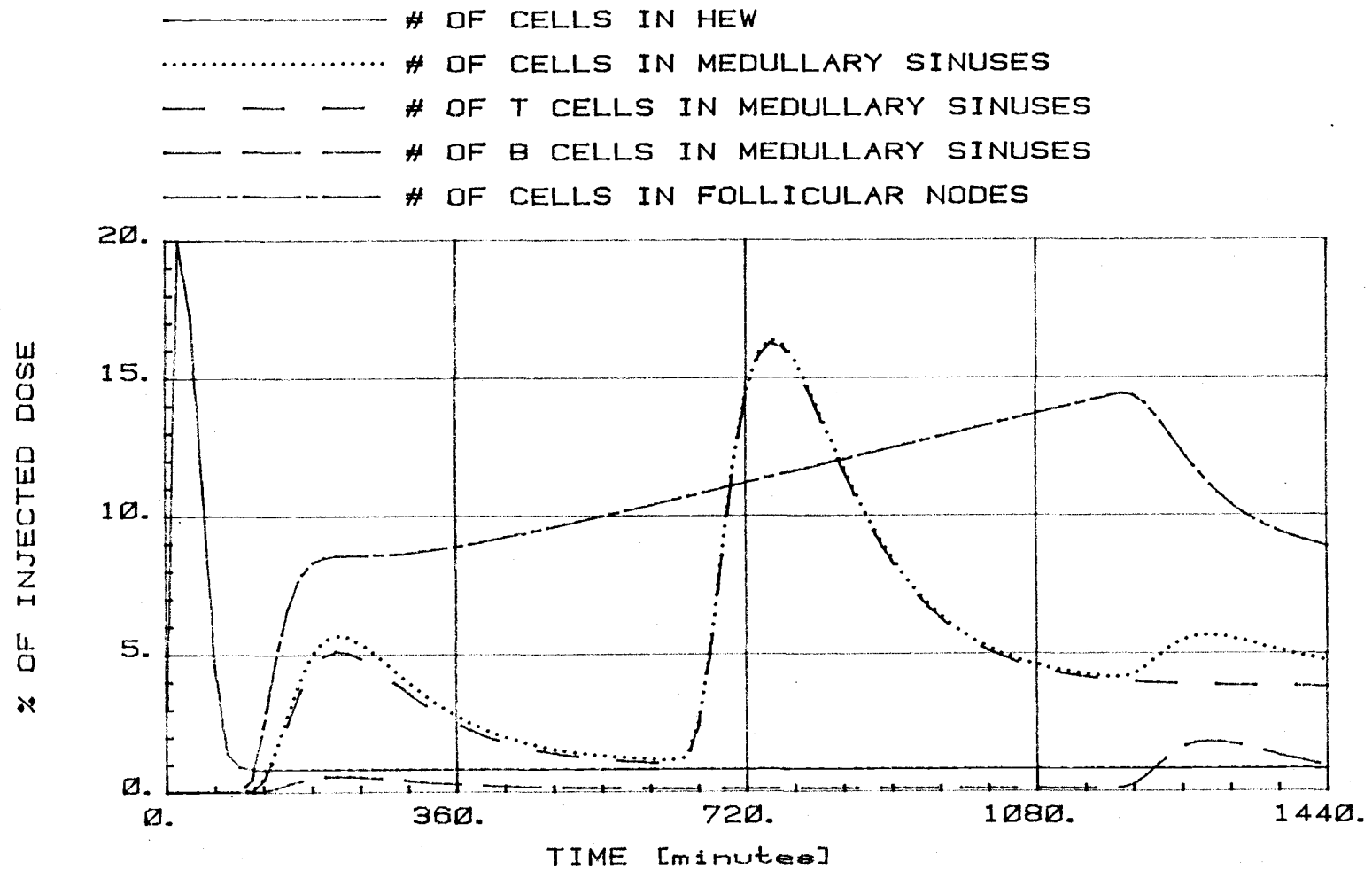


Figure 25b Simulation results II for linear decreasing input with constant limit value

A complete sensitivity analysis for the parameters was not performed for this model. Some effects of parameter variations however have already been discussed. It has been stated before that several parameters have little effect on the total number of cells in the node. This should not be confused with the statement that these parameters have little effect on the model. A parameter which has little effect on a model indicates redundancy and implies thereby that the model could be simplified. In fact, a far less elaborate model could be found if one is concerned only with input-output kinetics of a node. Such a model has already been proposed by Mohler et.al. [50]. The goal of this study however is an examination of different regions within a node and the constants mentioned above do have a decisive influence on the distribution of cells and are therefore not redundant. A further reduction of the model is not possible without losing some of its information content. The essential stations for lymphocyte migration through a lymphnode have been modeled with not more than two compartments per region and cell-type.

TABLE 3

Parameter values

$$Q_{bl} = 1.23 \text{ [ml/min]}$$

$$R_{bl-hw} = 0.25$$

$$R_{hw-ii} = 0.125$$

$$R_{ii-pn} = R_{ii-fn} = 0.05$$

$$R_{pn-ms} = R_{fn-ms} = 0.085$$

$$R_{ms-el} = 0.022$$

$$T_{ii} = 90 \text{ [min]}$$

$$T_{pn} = 540 \text{ [min]}$$

$$T_{fn} = 1080 \text{ [min]}$$

$$fd = 0.7$$

VI. CONCLUSION

Experimental verification of the proposed model has to be the next step. As it has already been stated, it is very difficult to measure lymphocyte dynamics within the compartments of a lymphnode. However, some of the necessary information can be extracted from more easily measurable steady state data. Further experimentation should include a detailed examination of the distribution of lymphocytes in different regions of a node after blood concentration has been held constant for at least 24 hours. It is important to note that the input function to a node is actually composed of three different functions, specifically the concentration of cells in blood, the blood flow rate and the rate constant at which lymphocytes enter the node. This rate constant as well as the blood flow rate are assumed to be constant in this model while the only varying input is the concentration of lymphocytes in blood. All three values have to be controlled during an experiment to draw valid conclusions from this model.

From the simulation, we can see that a promising experiment is the injection of a short bolus of labeled lymphocytes into the afferent bloodstream of a node and a subsequent examination of the efferent lymph of the node.

It has been common practice to examine thoracic duct lymph during a tracer experiment. The cell output in thoracic duct lymph however is a superposition of the characteristic response of many lymphnodes at different times. Much of the information content is lost due to this superposition. For this reason the output of a single node should be observed rather than the cell content of the thoracic duct.

Complete monitoring of the output of an individual lymphnode will result in detailed information about the kinetic behavior of the node. The model predicts three distinct peaks in the output of cells into efferent lymph. The first peak contains information about cells that cross the node without being immobilized for a longer time in paracortical nodules or follicular nodes. Transit time of cells across interfollicular interstitium can be found from this part of the output curve. The second peak will give the average transit time of T cells across a node as well as information about the ratio of delayed versus non-delayed T cells if compared in size to the first peak. The third and smallest peak contains information about the transit of B cells through the node. An important result will be the spread around the peak values. It will be crucial in determination of the validity of this model. If the spread is very large, the adoption of discrete time-delays will be a non-valid

approximation.

An extension of the proposed model seems promising and is rather easy to implement, as soon as more experimental data is available. Wide ranging conclusions can be drawn if the model is found valid and the proposal of an 'average' lymphnode can be accepted. An example is the analysis of data for coeliac lymphnodes from Smith and Ford's experiment. The kinetic behavior of coeliac nodes followed the pattern of other nodes except that it was significantly higher at all times. This model would explain this effect by a higher concentration of lymphocytes in inflowing blood, probably due to the fact that that the blood supply for coeliac nodes comes from the liver (Figure 4).

A mathematical model has been constructed that predicts the dynamics of lymphocyte migration through single lymphnodes. Based on simulation results, a new experiment was designed to obtain sufficient data for a better description of lymphocyte migration kinetics. The model can also be used as a building-block in a large-scale study of the complete immune system as shown in Figure 4. A detailed model of this kind that is based on previously derived subunits would be a big step forward in the ongoing search to understand the effects of the immune system. Development of such a model may

eventually have an impact on disease control and cancer research by effectively relating control theory and immunotherapy. Systems theory has been proven to be an important and useful tool to reduce the infinite complexity of living things to its essential mechanisms and thereby make it possible to understand the concepts and the structural framework of physical processes in general and the immune response in particular.

BIBLIOGRAPHY

- [1] Anderson,A.O. and Anderson,N.D., "Lymphocyte emigration from high endothelial venules in rat lymph nodes", Immunology, Vol.31, pp.731-748, 1976
- [2] Andrews,P., Milson,D.W. and Ford,W.L., "Migration of lymphocytes across specialized vascular endothelium V. Production of a sulphated macromolecule by high endothelial cells in lymphnodes", J.Cell.Sci., Vol. 57, pp.277-299, 1982
- [3] Bell,G.I., "Mathematical model of clonal selection and antibody production", J.Theoret.Biol., Vol. 29, pp.191-232, 1970
- [4] Bell, G.I., Part II, "mathematical model of clonal selection and antibody production", J.Theoret Biol., Vol. 33, pp.339-378, 1971
- [5] Bell,G.I., Part III,"The cellular basis of immunological paralysis", J.Theoret. Biol., Vol. 33, pp.379-398, 1971
- [6] Bell,G.I., Perelson,A.S. and Pimbley,G.H. Eds., Theoretical Immunology, Marcel Dekker, New York 1978
- [7] Brown,R.F., "Compartmental system analysis: state of the art", IEEE Trans. Biomed. Eng., Vol. BME-27, pp.1-11, 1980
- [8] Bruni,C, Giovenco,M.A., Koch,G. and Strom,R., "A dynamical model of humoral immune response", Math. Biosc., Vol.27, pp.191-227, 1975
- [9] Bruni,C., Giovenco,M.A., Koch,G. and Strom,R., "Modeling of the immune response: A system approach", in [6] , pp.379-414, 1978
- [10] Burnet,F.M., The clonal selection theory of acquired immunity , Vanderbilt and Cambridge University presses, Nashville,TN and London, England, 1959
- [11] Cahill,P.N., Frost,H. and Trnka,Z., "The effects of antigen on the migration of recirculating lymphocytes through single lymphnodes", J.Exp.Med., Vol.143, pp.870-888, 1976

- [12] Cahill, P.N., Poskitt, D.C., Frost, H. and Trnka, Z., "Two distinct pools of recirculating T lymphocytes: migratory characteristics of nodal and intestinal T lymphocytes", J.Exp.Med., Vol.145, pp.420-428, 1977
- [13] Cottier, H. Hess, M.W., Keller, H.-U., "Structural basis for lymphoid tissue functions: established and disputable sites of antigen-cell and cell-to-cell interactions in vivo", Monographs in Allergy, Vol.16, pp.50-71, 1980
- [14] Dibrov, B.F., Livshits, M.A. and Volkenstein, M.V., "Mathematical model of immune response", J. Theor. Biol., Vol.65, pp.609-631, 1977
- [15] Drayson, M.T., Smith, M.E. and Ford, W.L., "The sequence of changes in blood flow and lymphocyte influx to stimulated rat lymphnodes", Immunology, Vol.44, pp.125-133, 1981
- [16] Driver, R.D., "Ordinary and delay differential equations", Series Applied Mathematical Sciences, Vol. 20, Springer-Verlag, New York 1977
- [17] Ewijk, W., Brons, N.H.C. and Rozing, J., "Scanning electron microscopy of homing and recirculating lymphocyte populations", Cell.Immun., Vol.19, pp.245-261, 1975
- [18] Fahy, V.A., Gerber, H.A., Morris, B., Trevella, W. and Zukoski, C.F., "The function of lymphnodes in the formulation of lymph", Monographs in allergy, Vol.16, pp.82-99, 1980
- [19] Ford, W.L. and Simmons, S.J., "The tempo of lymphocyte recirculation from blood to lymph in the rat", Cell.Tiss.Kinet., Vol.5, pp.175-189, 1972
- [20] Fossum, S., "The architecture of rat lymphnodes, II. Lymphnode compartments", Scand.J.Immun., Vol.12, pp.411-420, 1980
- [21] Fossum, S., Smith, M.E. and Ford, W.L., "The migration of lymphocytes across specialized vascular endothelium VII. The migration of T and B lymphocytes from the blood of the athymic, nude rat", Scand.J. Immun., Vol.17, pp.539-549, 1983
- [22] Fossum, S., Smith, M.E. and Ford, W.L., "The recirculation of T and B lymphocytes in the athymic nude rat", Scand.J.Immun., Vol.17, pp.551-557, 1983
- [23] Frost, H., "The effect of antigen on the output of

- recirculating T and B lymphocytes from single lymphnodes", Cell.Immun., Vol.37, pp.390-396, 1978
- [24] Frost,H., Cahill,R.N.P. and Trnka,Z., "The migration of recirculating autologous and allogenic lymphocytes through single lymphnodes", Eur.J.Immun., Vol.5, pp.839-843 1975
- [25] Goldschneider,I. and McGregor,D.D., "Migration of lymphocytes and thymocytes in the rat, I. The route of migration from blood to spleen and lymph nodes", J.Exp.Med., Vol.127, pp.155-167, 1968
- [26] Goldschneider,I. and McGregor,D.D., "Anatomical distribution of T and B lymphocytes in the rat, Development of lymphocyte-specific antisera", J.Exp.Med., Vol.138, pp.1443-1465, 1973
- [27] Gowans,J.L., "The recirculation of lymphocytes from blood to lymph in the rat", J.Physiol., Vol.146, pp.54-69 1959
- [28] Gowans,J.L. and Knight,E.J., "The route of recirculation of lymphocytes in the rat", Proc.Roy.Soc.B, Vol.159, pp.257-282, 1964
- [29] Gutman,G.A. and Weissman,I.L., "Homing properties of thymus-independent follicular lymphocytes", Transplantation, Vol.16, pp.621-629, 1973
- [30] Guyton,A.C., Textbook of medical physiology, Philadelphia: W.B.Saunders Company, Philadelphia 1971
- [31] Hall,J.G. and Morris,B., "The output of cells in lymph from the popliteal node of the sheep", Q.J.Exp.Physiol., Vol.47, pp.360-369, 1962
- [32] Hall,J.G. and Morris,B., "The origin of the cells in the efferent lymph from a single lymph node", J.Exp.Med., Vol.121, pp.901-910 1965
- [33] Hammond,B.J., "A compartmental analysis of circulatory lymphocytes in the spleen", Cell.Tiss.Kinet., Vol.8, pp.153-169 1975
- [34] Hege,J.S. and Cole, J.L., "Mathematical model relating circulating antibody and antibody forming cells", J.Immunol., Vol. 94, pp.34-40, 1966
- [35] Howard,J.C., Hunt,S.V. and Gowans J.L., "Identification of marrow-derived and thymus-derived small lymphocytes in the lymphoid tissue and

- thoracic duct lymph of normal rats", J.Exp.Med., Vol.135, pp.200-219, 1972
- [36] Jacquez,J.A., Compartmental analysis in biology and medicine, New York 1972
- [37] Jilek,M. and Sterzl,J., "Modeling of the immune response", in Morphological and functional aspects of immunity, pp.333-349, Plenum Press, New York 1971
- [38] Jilek,M., "Immune response and its stochastic theory", Proc. IFAC Symposium on system identificatoin, The Hague, pp.209-212, 1973
- [39] Kelly,R.H., "Localization of afferent lymph cells within the draining node during a primary immune response", Nature, Vol.227, pp.510-513, 1970
- [40] Leeson,C.R. and Leeson,T.s., Histology, Third edition, pp.271-280, W.B.Saunders Co., Philadelphia 1976
- [41] Marchuk,G.I., Mathematical models in immunology, Springer Verlag, New York 1984
- [42] McConnel,I. and Hopkins,J., "Lymphocyte traffic through antigen-stimulated lymphnodes, I. Complement activation within lymph nodes initiates cell shutdown", Immunology, Vol.42, pp.217-231, 1981
- [43] MacDonald,N., "Time lags in biological models", Series Lecture Notes in Biomathematics, Vol. 27, Springer Verlag, Berlin 1978
- [44] Mohler,R.R., "Biological modeling with variable compartmental structure", IEEE Trans. Automat. Control, Vol. AC-19, pp.922-926, 1974
- [45] Mohler,R.R. and Barton, C.F., "Compartmental control model of the immune process", in Proc. 8th IFIP Optimization Conf. (Wuerzburg, Germany) Springer Verlag, New York 1977
- [46] Mohler,R.R. and Hsu,C.S., "Systems compartmentation in immunological modeling", in Proc. Rome Conf. System Theory in Immunology, Springer Verlag, New York 1978
- [47] Mohler,R.R., Barton,C.F. and Hsu, C.S., "T and B cells in the immune system", in [6], pp.415-436, 1978
- [48] Mohler,R.R. and Hsu, C.S., T-B cell control

- processes in immunology", in Proc. IEEE and SIAM Decision and Control Conf., San Diego, Cal. 1979
- [49] Mohler, R.R., Bruni, C. and Gandolfi, A., "A systems approach to immunology", Proceedings of the IEEE, Vol.68, pp.964-990, 1980
- [50] Mohler, R.R., Farooqi, Z. and Heilig, T. "An immune lymphocyte circulation model", To be published
- [51] Newman, E.V., Merrel, M., Genecin, A., Monge, C., Milnor, W.R. and McKeever, W.P., "The dye dilution method for describing the central circulation. An analysis of factors shaping the time concentration curves", Circulation, Vol.4, pp.735-746, 1951
- [52] Nieuwenhuis, P. and Ford, W.L., "Comparative migration of B and T lymphocytes in the rat spleen and lymph nodes", Cell.Immun., Vol.23, pp.254-267, 1976
- [53] Parrot, D.M.V., DeSousa, M.A.B. and East, J., "Thymus-dependent areas in the lymphoid organs of neonatally thymectomized mice", J.Exp.Med., Vol.193, pp.191-203, 1966
- [54] Sedgley, M. and Ford, W.L., "The migration of lymphocytes across specialized vascular endothelium, I. The entry of lymphocytes into the isolated mesenteric lymph node of the rat", Cell.Tiss.Kinet., Vol.9, pp.231-243, 1976
- [55] Sheppard, C.W., "The theory of the study of transfers within a multi-compartment system using isotopic tracers", J.Appl.Phys., Vol.19, pp.70-76, 1948
- [56] Sheppard, C.W. and Householder, A.S., "The mathematical basis of the interpretation of tracer experiments in closed steady-state systems", J.Appl.Phys., Vol.22, pp.510-520, 1951
- [57] Sheppard, C.W., Basic principles of the tracer method, New York, 1962
- [58] Smith, M.E. and Ford, W.L., "The recirculating lymphocyte pool of the rat: a systematic description of the migratory behaviour of recirculating lymphocytes", Immunology, Vol.49, pp.83-94, 1983
- [59] Smith, M.E. and Ford, W.L., "The migration of lymphocytes across specialized vascular endothelium VI. The migratory behaviour of thoracic duct lymphocytes re-transferred from the lymph nodes,

spleen blood or lymph of a primary recipient"
Cell.Immunol. Vol.78, pp.161-173, 1983

- [60] de Sousa, M., Lymphocyte circulation, John Wiley & Sons, Chichester (England) 1981
- [61] Trevella, W. and Morris, B., "The reassortment of cell populations within the lymphoid apparatus of the sheep", CIBA Foundation Symposium, 1979
- [62] Weissman, I.L., Gutman, G.A. and Friedberg, S.H., "Tissue localization of lymphoid cells", Ser. Haemat., Vol.7, pp.482-504, 1974
- [63] Yoffey, J.M. and Courtice, F.C., Lymphatics, lymph and the lymphomyeloid complex, Academic Press, London 1970